cholesterol, BIT9500 (StemCell Technologies Inc.), and Iscove's modified Dulbecco's medium. The cells were cultured for 12 d at 37°C. The cells were collected and stained with anti-human CD41-FITC (BD PharMingen, San Diego, CA, USA). After incubation for 20 min at 4°C, cells were washed, made permeable by gradual addition of methanol which was chilled at −40°C, and incubated for 30 min at 4°C. Then, cells were treated with 100 μg/mL RNase (Nippon Gene, Toyama, Japan) for 30 min at 4°C, and 50 μg/mL propidium iodide (PI) (Sigma, St. Louis, MO, USA) was added. After incubation for 30 min under darkness at 4°C, the cells were suspended in 500 μL of 2% FBS-PBS and analyzed using a flow cytometry (EPICS XL-MCL, Beckman-Coulter, Miami, FL, USA). Cells expressing CD41 were regarded as megakaryocytes. Ploidy distribution was analyzed by histogram. Events of each peak were counted by setting markers. Each ploidy level was expressed as event %. Event % at ploidy level of nN was calculated by the followed equation; Events % (nN) = [nN/(2N + 4N + 8N + 16N + 32N<)] × 100.

Western blot analysis of signal transduction through TPO receptor

Human TPO receptor expressing Ba/F3 cells washed free of growth factors by media, were incubated in RPMI1640 supplemented with 10% FBS and 50 units/mL penicillin/streptomycin for 15 h at 37°C. After this depletion period, cells were resuspended in RPMI1640 at a concentration of 1×10^6/mL and were stimulated with either AKR-501 or rhTPO at 37°C for 15 min. Cells were lysed in the same volume of a buffer containing 15 mM HEPES (pH 7.4), 150 mM NaCl, 10 mM EGTA, 1 mM sodium orthovanadate, protease inhibitor cocktail tablet (Roche Diagnostics, Indianapolis, IN, USA), and 2% (w/v) Triton X-100. Insoluble materials were removed by centrifugation at 10 000 × *g* for 30 min at 4°C. Total lysates were separated by electrophoresis using an SDS-PAGE gel under reducing conditions and transferred to a sheet of polyvinylidene difluoride membrane (Millipore, Bedford, MA, USA). The membrane was then blocked with Block Ace (Dainihon-Seiyaku, Osaka, Japan) at room temperature for 30 min. Membranes were then incubated overnight at 4°C in a hybridization buffer consisting of anti-phospho-STAT3 (Tyr705), anti-phospho-STAT5 (Tyr694), and anti-phospho-ERK (Thr202, 204) antibodies (Cell Signaling, Beverly, MA, USA) in Tris-buffered saline with 0.05% Tween 20 (TBST), and 3% FBS. These filters were stripped and reprobed with anti-STAT3, anti-STAT5 (Santa Cruz Biotechnology, CA, USA), and anti-ERK antibodies (Upstate Biotechnology, Lake Placid, NY, USA) to assure equal loading in each lane of the gel. Blots were developed using an ECL kit (Amersham Pharmacia, Buckinghamshire, UK).

Western blot analysis of tyrosine phosphorylation of STAT 5 in the platelets

Human blood was drawn from healthy volunteers in the presence of a 1/10th volume of 3.8% sodium citrate, added as an anticoagulant, and centrifuged at 150 × *g* for 10 min to obtain platelet-rich plasma (PRP). Animal blood from various species (chimpanzee, olive baboon, rhesus monkey, cynomolgus monkey, common marmoset, squirrel monkey, beagle dog, guinea pig, rabbit, rat, and hamster) were drawn in the presence of 1/10th volume of 3.8% sodium citrate. PRP was prepared by centrifugation of whole blood at 170 × *g* for 10 min. After the addition of 5 nM PGE_1 (Sigma), 5 mM EDTA (pH 8.05), and 3 U/mL apyrase (Sigma), the PRP was centrifuged at 1490 × *g* to form a platelet pellet. The pellet was resuspended in 5 mL of a Tyrode's-HEPES buffer (137 mM NaCl, 2.68 mM KCl, 3.75 mM NaH_2PO_4, 0.98 mM $MgCl_2$, 5.55 mM dextrose, 0.35% (w/v) BSA, and 37.8 mM HEPES, pH 6.7) also containing 5 nM PGE_1, 5 mM EDTA (pH 8.05), and 3 U/mL apyrase and washed once. For western blot analysis, platelets were resuspended at a concentration of 3×10^8 cells/mL in the Tyrode's-HEPES buffer (pH 7.35) and were stimulated with either AKR-501 or rhTPO at 37°C for 15 min. The Western blot protocol was as described above. In the incubation process, membranes were in a hybridization buffer consisting of anti-phospho-STAT5 antibody in TBST and 3% FBS.

Transplantation of human fetal liver $CD34^+$ cells into NOD/SCID mice

Human fetal liver (FL) $CD34^+$ cells (approximately 1 00 000 cells/mouse, BioWhittaker Inc, Walkersville, MD, USA) were injected into 9- to 12-wk-old NOD/SCID mice through the tail vein after irradiation with 2.4 Gy as two divided doses at intervals of at least 4 h by an X-ray apparatus (MBR-1520R-3, Hitachi Medical Corporation, Tokyo, Japan). The transplanted mice were injected intraperitoneally with anti-asialo GM1 antiserum (Wako, Osaka, Japan) immediately before cell transplantation and every 9–11 d after cell transplantation, a total of six times in order to deplete natural killer cells. After transplantation, mice were given sterile water containing prophylactic neomycin. Peripheral blood (PB) was obtained from the retro-orbital plexus using heparinized calibrated pipets (Drummond Scientific Co, Broomall, PA, USA), and transferred to EDTA 2Na containing Capiject (Terumo Medical, Somerset, NJ, USA). Blood cell counts were measured

using an automatic cell counter (MEK-6258, Nihon Kohden, Tokyo, Japan).

Flow cytometric analysis of peripheral blood in transplanted NOD/SCID mice

Human platelets from NOD/SCID mice were analyzed by flow cytometry (EPICS XL-MCL). Human platelets in PB were measured by staining with anti-human CD41-PE and anti-murine CD41-FITC (BD PharMingen). The percentage of human platelets was calculated by dividing the number of $hCD41^+$ cells by the total number of $CD41^+$ cells (human and mouse). The number of human platelets in PB was calculated by multiplying the percentage of human platelets by the total blood platelet count in PB, as measured with an automatic cell counter. The number of murine platelets in PB was calculated by subtracting the number of human platelets from the total platelet count.

Administration of AKR-501 to transplanted NOD/SCID mice

Various doses of AKR-501 (0, 0.3, 1, and 3 mg/kg/d), suspended in 0.5% methylcellulose, were orally administered for 14 d to NOD/SCID mice transplanted with human FL $CD34^+$ cells. PB was collected on days 7, 14, 21, and 28 after the start of AKR-501 administration, and blood cell counts and the number of human platelets were measured. The time course of changes in human and murine platelets number is expressed in terms of the rate of increase after administration of AKR-501 relative to the value at predosing. Statistical analysis was performed by Dunnett's test.

Results

AKR-501 is a TPO receptor agonist

We screened for small molecule compounds that mimic the action of TPO using a method that measured the proliferative activity of human TPO receptor-expressing Ba/F3 cells, resulting in the discovery of an orally active TPO receptor agonist, AKR-501. AKR-501 supported the proliferation of TPO receptor expressing Ba/F3 cell in a concentration-dependent fashion (Fig. 1A). The compound demonstrated an EC_{50} value of 3.3 ± 0.2 nM in this assay with the maximum proliferative activity equivalent to maximum activity of rhTPO. The activity of the compound was dependent on the TPO receptor, because parental Ba/F3 cells did not respond to either AKR-501 or rhTPO (Fig. 1A, B). Further, AKR-501 induced tyrosine phosphorylation of STAT3 and STAT5, and threonine phosphorylation of ERK in the cells, as did rhTPO. Thus, AKR-501 activates signal transduction in TPO receptor expressing Ba/F3 cells through the TPO receptor, and supports the proliferation of these cells (Fig. 1C).

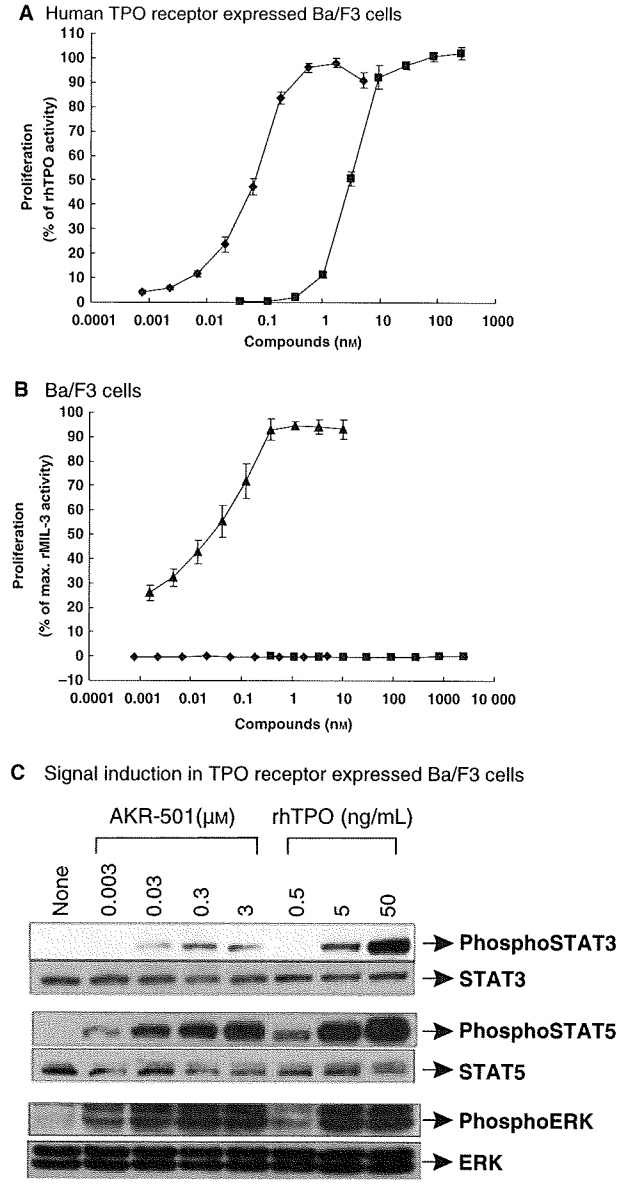

Figure 1 AKR-501 specifically acts on human Thrombopoietin (TPO) receptor. (A, B) Proliferative response of human TPO receptor expressed Ba/F3 cells (A) and Ba/F3 cells (B) to AKR-501 (■), rhTPO (♦), and rmIL-3 (▲). Data are presented as mean ± SE (n = 5). (C) Signal induction in TPO receptor expressed Ba/F3 cells. Human TPO receptor expressed Ba/F3 cells were stimulated by AKR-501 or rhTPO. Immunoblots were probed with anti-phospho-STAT3, anti-phospho-STAT5, and anti-phospho-ERK antibodies. These filters were stripped and reprobed with anti-STAT3, anti-STAT5, and anti-ERK antibodies.

TPO specifically stimulates megakaryocytopoiesis throughout the development and maturation of

megakaryocytes. Therefore, we examined the effect of AKR-501 on the differentiation to megakaryocytes from hematopoietic progenitor cells. AKR-501 promoted megakaryocyte colony formation from human CB $CD34^+$ cells in a concentration-dependent fashion (Fig. 2A). The EC_{50} value was 25.0 ± 7.8 nM for AKR-501 and the maximum activity of AKR-501 was similar to that of rhTPO. Human megakaryocyte colonies generated with AKR-501 and rhTPO had similar morphologic features (Fig. 2B, C). Further, AKR-501 and rhTPO induced polyploidization of megakaryocytes from G-CSF mobilized peripheral blood $CD34^+$ cells in liquid culture (Fig. 3A, B). There was no apparent difference between AKR-501 and rhTPO at each ploidy level (Fig. 3C). These results suggest that AKR-501 mimics the effect of TPO *in vitro*.

Species specificity of AKR-501

TPO receptor is expressed on the surface of platelets, and TPO induces signal transduction including STAT5. The species specificity of AKR-501 for the TPO receptor was demonstrated by STAT5 activation in platelets of various species (Fig. 4). AKR-501 induced tyrosine phosphorylation of STAT5 in human blood platelets and chimpanzee blood platelets, as did rhTPO. In contrast, rhTPO induced tyrosine phosphorylation of STAT5 in olive baboon, cynomolgus monkey, rhesus monkey, common marmoset, squirrel monkey, beagle dog, guinea pig, rabbit, rat, and hamster platelets (data not shown), but AKR-501 did not induce phosphorylation in these species.

Evaluation of AKR-501 on human platelet production in NOD/SCID mice

AKR-501 was shown to have strict species-specificity and to be effective only in humans and chimpanzees. To examine the *in vivo* pharmacological effects of AKR-501 on human platelet production, we used NOD/SCID mice transplanted with FL $CD34^+$ cells. NOD/SCID mice were characterized as an efficient engraftment model for HSCs. It had been reported that the multilineages of human hematopoiesis, including the production of human platelets, could be reconstituted over a long period of time in NOD/SCID mice transplanted with human HSCs (13, 14). In this study, we used commercially available cryopreserved human FL $CD34^+$ cells as a source of HSCs.

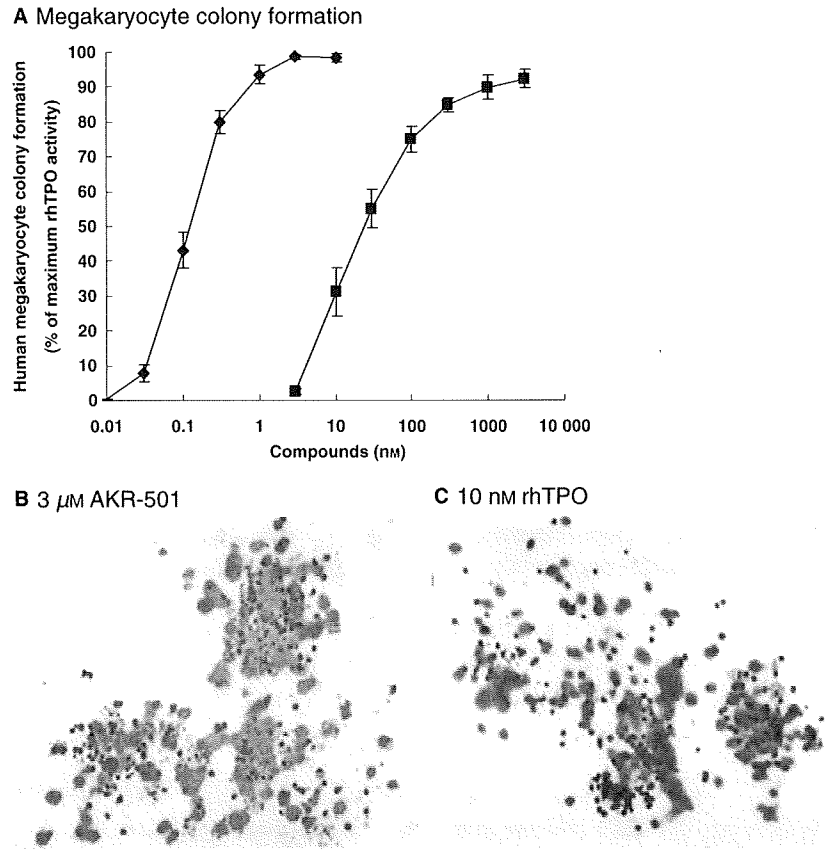

Figure 2 AKR-501 promotes megakaryocyte differentiation from human $CD34^+$ cells. (A) Megakaryocyte colony formation was measured in serum-free collagen-based medium cultures of human cord blood $CD34^+$ cells in the presence of increasing concentrations of AKR-501 (■), and recombinant human TPO (rhTPO) (♦). Data are presented as mean ± SE (n = 5). (B, C) Immunohistochemical identification of typical human megakaryocyte colonies generated with 3 μM AKR-501 (B) and 10 nM rhTPO (C) × 100 objectives.

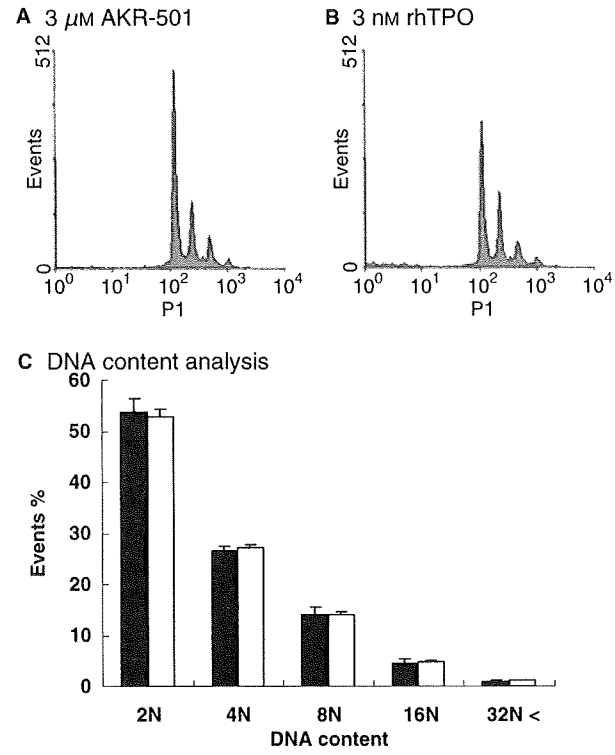

Figure 3 AKR-501 induces polyploidization of megakaryocytes. G-CSF-mobilized human peripheral blood $CD34^+$ cells were cultured for 12 d in serum-free liquid medium in the presence of 3 μM AKR-501 or 3 nM recombinant human TPO (rhTPO). Following surface marker staining, DNA analysis was performed by staining with propidium iodide. The plots show the typical ploidy distribution after gating on $CD41^+$ cells (A: 3 μM AKR-501, B: 3 nM rhTPO). (C) Ploidy analysis of megakaryocytes generated by 3 μM AKR-501 (open columns) or 3 nM rhTPO (filled columns). The data represent the mean ± SE of five independent experiments. Statistical analysis was performed in each DNA content group using Student's *t*-test.

Human platelets started to appear in the PB of these mice 4 wk after transplantation. The production of human platelets continued for more than 6 months post-transplant.

Doses of 0.3, 1, and 3 mg/kg/d of AKR-501 were orally administered once per day for 14 d to NOD/SCID mice that stably produced human platelets. Oral administration of AKR-501 dose-dependently increased the number of human platelets, resulting in approximately a 2.7-fold increase at 1 mg/kg/d ($P < 0.05$) and a 3.0-fold increase ($P < 0.01$) at 3 mg/kg/d on day 14 after the start of administration (Fig. 5A). The minimum effective dose was 1 mg/kg/d. Withdrawal of AKR-501 administration caused the human platelet count to return nearly to pretreatment levels. As was expected given the species selective activity of AKR-501, the murine platelet count did not change after oral administration of AKR-501 at any dosage (Fig. 5B). Further, WBC, RBC, and body weight did not significantly change during the study period (data not shown).

Discussion

We successfully employed high throughput screening techniques based on proliferation of human TPO receptor-expressing Ba/F3 cells to identify a series of 2-acylaminothiazole derivatives as a potent novel series of TPO receptor agonists. The lead agent in the series, AKR-501, caused dose-dependent proliferation of human TPO receptor-expressing Ba/F3 cells and promoted differentiation to human megakaryocytes. This agent was efficacious following oral administration, producing a dose-dependent increase of human platelet numbers in NOD/SCID mice transplanted with human FL $CD34^+$ cells.

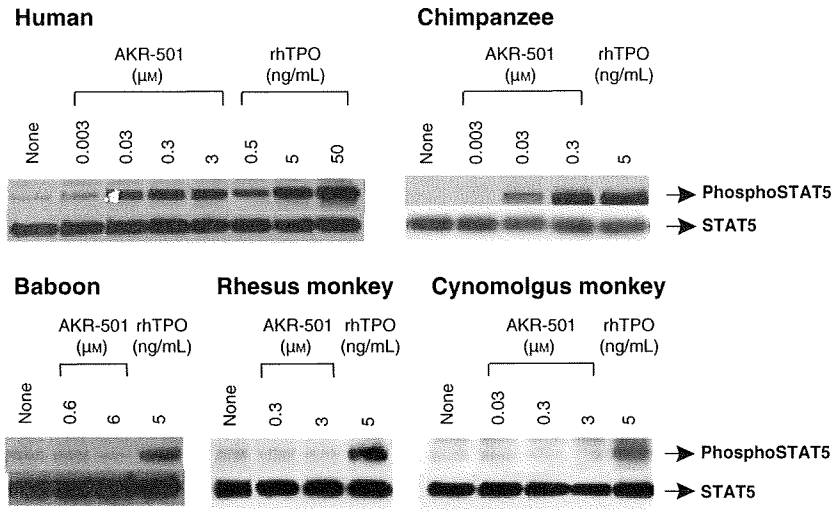

Figure 4 AKR-501 activates STAT5 in human and chimpanzee platelets, but not in baboon, rhesus, and cynomolgus monkey platelets. Human and non-human primate platelets were stimulated by AKR-501 or recombinant human TPO (rhTPO). Immunoblots were probed with anti-phospho-STAT5 antibody. These filters were stripped and reprobed with anti-STAT5 antibody.

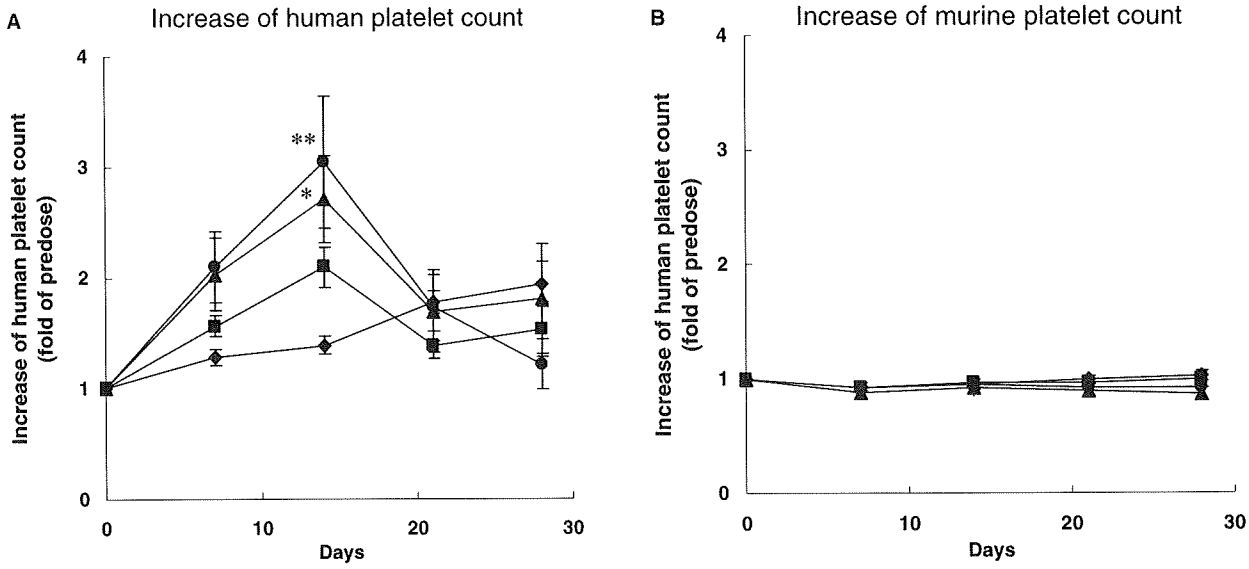

Figure 5 Oral administration of AKR-501 increases the number of human platelets in NOD/SCID mice transplanted with human FL CD34$^+$ cells. AKR-501 (vehicle (♦), 0.3 (■), 1 (▲), and 3 (•) mg/kg/d) was orally administered for 14 d to human platelet-producing NOD/SCID mice. PB was collected on the indicated days, and blood cell counts were measured. The percentage of human platelets was measured by flow cytometry, and the number of human (A) and murine platelets (B) was calculated as described in 'Materials and methods'. The time course of changes in human and murine platelet count is expressed in terms of the fold increase after administration of AKR-501 relative to the value at predosing. Data are presented as mean ± SE (n = 10, on day 28; n = 9 for vehicle, 0.3, 3 mg/kg/d groups). *$P < 0.05$, **$P < 0.01$ vs. vehicle group by Dunnett's test.

Other small molecules such as TM41 (15), SB-497115 (eltrombopag) (16), SB-394725 (17), and NIP-004 (18) have been reported as TPO receptor agonists. Some compounds including eltrombopag, SB-394725, and NIP-004 display species specificities (17–19) as did the compounds in our series. In order to identify an orally active TPO receptor agonist, we utilized NOD/SCID mice transplanted with human FL CD34$^+$ cells to evaluate hematopoietic stem cells (20–22) and human platelet production (13, 14). Previously we reported that subcutaneous injection of TPO to NOD/SCID mice transplanted with human cord blood CD34$^+$ cells dose-dependently increased the number of human platelets (14), and subcutaneous injection of NIP-004 has been shown to induce human platelet production in a xenotransplatation model (18). Herein we report that oral administration of AKR-501 to the NOD/SCID mice model increased the number of human platelets. To our knowledge, no other TPO agonists have been reported to be orally administered to the NOD/SCID mice model. Therefore, AKR-501 is the first TPO receptor agonist whose platelet increasing effect was proven by oral administration to NOD/SCID mice transplanted with human hematopoietic stem cells.

The efficacy of AKR-501 seen in the non-clinical model has also been demonstrated in the clinic. In a phase I study, once daily oral administration of AKR-501 at 10 mg to healthy volunteers for 14 d increased the number of platelets, resulting in a >50% increase over baseline platelet count (23). This result is consistent with the *in vivo* result using NOD/SCID mice transplanted with human FL CD34$^+$ cells. Furthermore, similar peak unbound plasma concentrations of AKR-501 were observed in both the non-clinical model and in this phase I clinical trial. The peak unbound plasma concentrations of AKR-501 after administration at 1 mg/kg in the NOD/SCID mice study and after 14 d dosing at 10 mg/d in human study were 3.3 and 3.4 ng/mL, respectively. The observed pharmacodynamic responses at comparable exposures demonstrate that the NOD/SCID model is suitable for predicting the concentration-effect relationship of orally-active TPO receptor agonists in man.

In conclusion, we identified a novel orally-active TPO receptor agonist, AKR-501, which mimics the biological activity of TPO both *in vitro* and *in vivo*. These non-clinical results and early results from clinical investigations suggest that AKR-501 is an orally active TPO receptor agonist that may prove useful for treating patients with thrombocytopenia.

Acknowledgements

We gratefully acknowledge Dr. Robert E. Desjardins for reviewing the manuscript and Dr. Stephen J. Waters for editing the manuscript.

Authorship

Contribution: M.F-S. performed research, analyzed data, and wrote the paper, K.Suzuki designed research, performed research, analyzed data and edited the paper, Y.I., M.A. and K.Sugasawa performed research, F.H. analyzed data, T.K. analyzed data and edited the paper, and T.N supervised the study.

Conflict-of-interest disclosure

Tatsutoshi Nakahata declares no competing financial interests. Other authors are employees of Astellas Pharma Inc.

References

1. Kaushansky K. Thrombopoietin. *N Engl J Med* 1998;**339**:746–54.
2. Kaushansky K, Drachman JG. The molecular and cellular biology of thrombopoietin: the primary regulator of platelet production. *Oncogene* 2002;**21**:3359–67.
3. Li J, Yang C, Xia Y, Bertino A, Glaspy J, Roberts M, Kuter DJ. Thrombocytopenia caused by the development of antibodies to thrombopoietin. *Blood* 2001;**98**:3241–8.
4. Basser RL, O'Flaherty E, Green M, Edmonds M, Nichol J, Menchaca DM, Cohen B, Begley CG. Development of pancytopenia with neutralizing antibodies to thrombopoietin after multicycle chemotherapy supported by megakaryocyte growth and development factor. *Blood* 2002;**99**:2599–602.
5. Vadhan-Raj S, Murray LJ, Bueso-Ramos C, *et al.* Stimulation of megakaryocyte and platelet production by a single dose of recombinant human thrombopoietin in patients with cancer. *Ann Intern Med* 1997;**126**:673–81.
6. Kuter DJ. New thrombopoietic growth factors. *Blood* 2007;**109**:4607–16.
7. Reiter LA, Subramanyam C, Mangual EJ, *et al.* Pyrimidine benzamide-based thrombopoietin receptor agonists. *Bioorg Med Chem Lett* 2007;**17**:5447–54.
8. Alper PB, Marsilje TH, Mutnick D, *et al.* Discovery and biological evaluation of benzo[a]carbazole-based small molecule agonists of the thrombopoietin (Tpo) receptor. *Bioorg Med Chem Lett* 2008;**18**: 5255–8.
9. Marsilje TH, Alper PB, Lu W, *et al.* Optimization of small molecule agonists of the thrombopoietin (Tpo) receptor derived from a benzo[a]carbazole hit scaffold. *Bioorg Med Chem Lett* 2008;**18**:5259–62.
10. Reiter LA, Jones CS, Brissette WH, *et al.* Molecular features crucial to the activity of pyrimidine benzamide-based thrombopoietin receptor agonists. *Bioorg Med Chem Lett* 2008;**18**:3000–6.
11. Duffy KJ, Darcy MG, Delorme E, *et al.* Hydrazinonaphthalene and azonaphthalene thrombopoietin mimics are nonpeptidyl promoters of megakaryocytopoiesis. *J Med Chem* 2001;**44**:3730–45.
12. Fukushima-Shintani M, Suzuki K, Iwatsuki Y, Abe M, Sugasawa K, Hirayama F, Kawasaki T. AKR-501 (YM477) in combination with thrombopoietin enhances human megakaryocytopoiesis. *Exp Hematol* 2008;**36**:1337–42.
13. Ueda T, Yoshino H, Kobayashi K, Kawahata M, Ebihara Y, Ito M, Asano S, Nakahata T, Tsuji K. Hematopoietic repopulating ability of cord blood CD34(+) cells in NOD/Shi-scid mice. *Stem Cells* 2000;**18**:204–13.
14. Suzuki K, Hiramatsu H, Fukushima-Shintani M, Heike T, Nakahata T. Efficient assay for evaluating human thrombopoiesis using NOD/SCID mice transplanted with cord blood $CD34^+$ cells. *Eur J Haematol* 2007;**78**:123–30.
15. Kimura T, Kaburaki H, Tsujino T, Ikeda Y, Kato H, Watanabe Y. A non-peptide compound which can mimic the effect of thrombopoietin via c-Mpl. *FEBS Lett* 1998;**428**:250–4.
16. Erickson-Miller C, Delorme E, Giampa L, *et al.* Biological Activity and Selectivity for Tpo Receptor of the Orally Bioavailable, Small Molecule Tpo Receptor Agonist, SB-497115. *Blood (ASH Annual Meeting Abstracts)* 2004;**104**:2912.
17. Erickson-Miller CL, DeLorme E, Tian SS, *et al.* Discovery and characterization of a selective, nonpeptidyl thrombopoietin receptor agonist. *Exp Hematol* 2005;**33**:85–93.
18. Nakamura T, Miyakawa Y, Miyamura A, Yamane A, Suzuki H, Ito M, Ohnishi Y, Ishiwata N, Ikeda Y, Tsuruzoe N. A novel nonpeptidyl human c-Mpl activator stimulates human megakaryopoiesis and thrombopoiesis. *Blood* 2006;**107**:4300–7.
19. Erickson-Miller CL, Delorme E, Iskander M, *et al.* Species Specificity and Receptor Domain Interaction of a Small Molecule TPO Receptor Agonist. *Blood (ASH Annual Meeting Abstracts)* 2004;**104**:2909.
20. Dick JE, Bhatia M, Gan O, Kapp U, Wang JC. Assay of human stem cells by repopulation of NOD/SCID mice. *Stem Cells* 1997;**15**:199–203.
21. Greiner DL, Hesselton RA, Shultz LD. SCID mouse models of human stem cell engraftment. *Stem Cells* 1998;**16**:166–77.
22. Dao MA, Nolta JA. Immunodeficient mice as models of human hematopoietic stem cell engraftment. *Curr Opin Immunol* 1999;**11**:532–7.
23. Desjardins RE, Tempel DL, Lucek R, Kuter DJ. Single and multiple oral doses of AKR-501 (YM477) increase the platelet count in healthy volunteers. *ASH Annual Meeting Abstracts* 2006;**108**:477.

Pediatr Blood Cancer 2009;53:1011–1015

Treatment of Children With Refractory Anemia: The Japanese Childhood MDS Study Group Trial (MDS99)

Daisuke Hasegawa, MD,[1]* Atsushi Manabe, MD,[1] Hiroshi Yagasaki, MD,[2] Yoshitoshi Ohtsuka, MD,[3] Masami Inoue, MD,[4] Akira Kikuchi, MD,[5] Akira Ohara, MD,[6] Masahiro Tsuchida, MD,[7] Seiji Kojima, MD,[2] and Tatsutoshi Nakahata, MD[8] on behalf of Japanese Childhood MDS Study Group

Background. Although hematopoietic stem cell transplantation (HSCT) is offered as a curative therapy for pediatric myelodysplastic syndrome (MDS), it may cause severe complications and mortality. Several reports have shown the efficacy of immunosuppressive therapy (IST) in adult patients with refractory anemia (RA), but its safety and efficacy remains to be fully elucidated in childhood RA. ***Procedure.*** Eleven children diagnosed with RA and enrolled on a prospective multicenter trial conducted by the Japanese Childhood MDS Study Group were eligible for analysis. If patients showed transfusion dependent or suffered from infection due to neutropenia, they received IST consisting of antithymocyte globulin (ATG), cyclosporine (CyA), and methylprednisolone (mPSL). ***Results.*** Eight children received IST, 2 received only supportive therapy, and one underwent HSCT without IST. Five (63%) of eight children who received IST showed hematological response. Of note, one patient showed the disappearance of monosomy 7 after IST. Responders were significantly younger than non-responders (29 months vs. 140 months; $P = 0.03$). No severe adverse events related to IST were reported in this study. Of 6 children with chromosomal abnormalities who received IST, four showed hematological response. The probability of failure-free and overall survival at 5 years was $63 \pm 17\%$ and $90 \pm 9\%$ respectively. ***Conclusion.*** IST is likely to be a safe and effective modality for childhood RA. Pediatr Blood Cancer 2009;53:1011–1015. © 2009 Wiley-Liss, Inc.

Key words: myelodysplastic syndrome; refractory anemia; children; immunosuppressive therapy

INTRODUCTION

Myelodysplastic syndrome (MDS) is a hematopoietic stem cell disorder and rarely occurs in childhood [1,2]. Refractory anemia (RA) is a subgroup of MDS with less than 5% of blasts in the bone marrow (BM) and little is known about childhood RA because of its rarity. European Working Group of MDS in Childhood (EWOG-MDS) retrospectively analyzed the clinical characteristics of children with RA [3]. They found that neutropenia and thrombocytopenia were more prominent than anemia [3,4] and karyotype had a strong impact on prognosis in children with RA [3]. Children with monosomy 7 were significantly more likely to progress to advanced disease and they recommended hematopoietic stem cell transplantation (HSCT) for this unfavorable group as early as possible, whereas, appropriate treatment for children with chromosomal abnormalities other than monosomy 7 and those with normal karyotypes remained to be determined.

Disturbance of the immune system may play a role in pathogenesis in some adults and children with RA [5–7]. Several reports have shown positive effects of immunosuppressive therapy (IST) in adult patients with RA [8–12]. The hematological response rate of IST was reported as 30–80% but IST could not restore the cytogenetic abnormalities or dysplastic features. Recently, EWOG-MDS reported the results of IST consisting of antithymocyte globulin (ATG) and cyclosporine A (CyA) in children with hypoplastic refractory cytopenia (RC) and normal karyotype or trisomy 8 who were thought as being at low risk of progression to advanced MDS [13]. However, the role of IST in children with RA has not been fully elucidated because the above study selected children with favorable predictive factors for a positive response to IST.

This study reports the outcome of 11 children with RA enrolled on a prospective multicenter trial (MDS99) conducted by the Japanese Childhood MDS Study Group, which applied IST with ATG and CyA to unselected patients who needed intervention.

DOI 10.1002/pbc.22121
Published online 4 June 2009 in Wiley InterScience (www.interscience.wiley.com)

PATIENTS AND METHODS

Patients

Eleven children younger than 16 years of age were enrolled onto MDS99 from September 1999 to March 2004. They were diagnosed as having RA according to the French-American-British (FAB) classification [14] and diagnosis was confirmed by the central review of morphology by two independent investigators [15]. Cytogenetic analysis of the bone marrow cells was performed in each institution. There were no patients who had undergone previous chemotherapy or radiotherapy, nor patients with a history of congenital bone marrow failure syndrome or aplastic anemia in the analysis. The study was approved by the Steering Committee of the Japanese Childhood MDS Study Group and the institutional review boards of the participating institutions or the equivalent organization. Informed consent was obtained from the guardians of the patients.

[1]Department of Pediatrics, St. Luke's International Hospital, Tokyo, Japan; [2]Department of Pediatrics, Nagoya University School of Medicine, Nagoya, Japan; [3]Department of Pediatrics, Hyogo College of Medicine, Nishinomiya, Japan; [4]Division of Hematology/Oncology, Osaka Medical Center and Research Institute for Maternal and Child Health, Izumi, Japan; [5]Division of Hematology-Oncology, Saitama Children's Medical Center, Iwatsuki, Japan; [6]First Department of Pediatrics, Toho University, Tokyo, Japan; [7]Department of Pediatrics, Ibaraki Children's Hospital, Mito, Japan; [8]Department of Pediatrics, Kyoto University, Kyoto, Japan

The authors report no potential conflicts of interest.

*Correspondence to: Daisuke Hasegawa, Department of Pediatrics, St. Luke's International Hospital, 9-1, Akashi-cho, Chuo-ku, Tokyo 104-8560, Japan. E-mail: hase-dai@umin.net

Received 4 February 2009; Accepted 27 April 2009

Treatment Protocol

Each patient with RA required repetitive bone marrow aspiration at 6–8 weeks intervals in order to confirm the diagnosis. If the disease was stable and blood transfusion was not required, patients were observed closely without any therapy. If patients showed transfusion dependent or suffered from infection due to neutropenia, IST was administered as follows: horse ATG (15 mg/kg/day) for 5 days as a slow intravenous infusion over 12 hr, CyA (6 mg/kg/day given orally as an initial dose, and the dose was adjusted to achieve a whole blood trough level of 100–200 ng/ml) was started on day 1 and continued until day 180, and methylprednisolone (mPSL; 2 mg/kg/day) was administered intravenously on days 1–7, then mPSL was administered orally and slowly tapered from day 8 to end on day 29. In this study, the use of G-CSF was not restricted. HSCT was recommended when a patient showed no response to IST and required further intervention because of cytopenia or progression to more advanced disease.

Evaluation and Statistical Analysis

Response to IST was evaluated at 6 months. Complete response (CR) was defined as a neutrophil count $>1.5 \times 10^9$/L, platelet count $>100 \times 10^9$/L, and hemoglobin (Hb) level of >11.0 g/dl. Partial response (PR) was defined as a neutrophil count $>0.5 \times 10^9$/L, platelet count $>20 \times 10^9$/L, and Hb level of >8.0 g/dl. When neither the CR nor the PR criteria were met, a patient was considered as no response (NR) to IST.

Mann–Whitney test and Fisher's exact test were applied to evaluate the differences between patients that responded to IST and those who did not. Failure-free survival (FFS) was calculated from the date of initiating IST to the date of treatment failure as follows; death, no response to IST at 6 months, HSCT, a second course of IST, acquisition of chromosomal abnormality, progression to advanced disease, or relapse. Overall survival (OS) was calculated from the date of diagnosis to the date of death or last follow-up. Both FFS and OS were estimated by the Kaplan–Meier method.

RESULTS

Patient Characteristics

Eleven children, 6 males and 5 females, were analyzed in this study (Table I). The median age at diagnosis was 67 months (range, 9 months to 15 years). Eight of 11 children had neutrophil counts of less than 1.5×10^9/L. All except 1 patient had Hb levels below 10 g/dl. Eight patients had platelet counts below 50×10^9/L. In total, one patient had anemia only, five had bi-cytopenia (anemia and neutropenia 2, anemia and thrombocytopenia 2, and neutropenia and thrombocytopenia 1), and five had pancytopenia at diagnosis. Since bone marrow biopsy specimen was available in only 6 of 11 cases, we determined cellularity by central pathological review from bone marrow smear rather than biopsy specimens and used a more suitable term, cell content, instead of cellularity in this report. Overall, there were only three patients in whom BM cell content was low. All patients showed dysplasia in multilineage series, which was compatible with the definition of refractory cytopenias with multilineage dysplasia (RCMD) in the World Health Organization (WHO) classification [16]. Data on the cytogenetic analyses at diagnosis were available for all patients. Karyotype was normal in three patients, and of the remaining eight patients, two had monosomy 7, two had trisomy 8, and four had other abnormalities; del (7)(q11), i(8)(q10), 20q-, and +der(1;19)(q10;q10). Of four patients in whom presence of paroxysmal nocturnal hemoglobinuria (PNH) cells was assessed by flow cytometry, none showed an expansion of PNH clone. Of five patients in whom data on HLA-DR was available, only one patient showed DR2 antigen, which is a broad antigen of DR15 and DR16.

TABLE I. Patients Characteristics

	Median (range)
Age	5y7m (9m to 15y5m)
Gender	M/F = 6:5
WBC ($\times 10^9$/L)	3.8 (1.1–12.5)
Neutrophil ($\times 10^9$/L)	0.94 (0.16–8.1)
PB blast (%)	0 (0)
Hb (g/dl)	6.2 (3.6–11.7)
Reticulocyte (%)	2 (1–44)
Reticulocyte ($\times 10^9$/L)	41.7 (12.3–572.0)
MCV (fl)	104 (84–123)
Plt ($\times 10^9$/L)	23.0 (3.0–117.0)
BM blast (%)	1.0 (0–4.8)
BM cell content	Low 3, normal 5, high 3
Chromosome	Normal/abnormal = 3:8
Cytopenia[a]	Anemia only 1, bi-cytopenia 5, pancytopenia 5

[a]Cut-off; neutrophils <1,500/μl, Hb < 10.0 g/dl, Plt < 50,000/μl.

Observation Without Intervention

Figure 1 shows the outcome of the 11 patients analyzed. Of 3 patients who initially received only supportive therapy, one with normal karyotype was still stable without therapy, one with trisomy 8 showed spontaneous improvement of anemia but the chromosomal abnormality remained. One with 20q- (UPN 046) showed stable disease for 2 years, but cytopenia deteriorated and IST was initiated at 968 days after diagnosis.

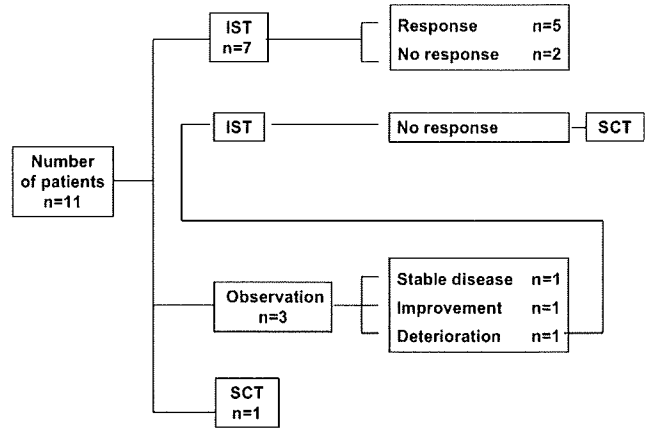

Fig. 1. Outcome of 11 patients with refractory anemia. SCT, stem cell transplantation; IST, immunosuppressive therapy.

Immunosuppressive Therapy

Seven patients received IST as the first-line treatment and one (UPN 046) received IST because of recurrence of cytopenia after 2-year observation. IST was given at a median of 42 (range 0–968) days after the diagnosis of RA. Five of eight patients showed response to IST at 6 months after the initiation of treatment (response rate was 63%; CR 2, PR3). Of five responders, three were able to successfully discontinue IST and remained disease-free, and the remaining two patients have been continuing therapy. Of note, the disappearance of a monosomy 7 clone after IST was observed in UPN 035 [17] and the patient is still in remission after 63 months. Of three non-responders, one was lost to follow up, one responded to a second course of IST, and one (UPN 046) underwent HSCT 3 months after initiating IST.

To address predictive factors for response to IST, the characteristics were compared between children who responded to IST and those who did not (Table II). The age at diagnosis was significantly younger in responders than in non-responders (median 29 months vs. 140 months; $P = 0.03$), whereas there was no statistically significant associations between response to IST and sex, neutrophil count, Hb level, platelet count, interval from diagnosis to IST, chromosomal abnormality, BM cell content, or number of cytopenia. Serious adverse events related to IST were not observed, including the progression to advanced disease. The most frequent adverse event in this study was pyrexia.

Hematopoietic Stem Cell Transplantation

Two children underwent HSCT in this series. One patient with 20q- (UPN 046) received bone marrow transplantation (BMT) from her human leukocyte antigen (HLA) 1-locus-mismatched father at 1,088 days after diagnosis because of non-response to IST. This patient suffered from adenoviral colitis, salmonella colitis, herpes zoster, and grade III acute GVHD of the skin, however, she is still alive without disease 23 months after BMT. One other patient with monosomy 7 (UPN 053) received BMT from a matched unrelated donor on 537 days after diagnosis without IST by physician's decision. His post-transplant course was uneventful, but disease relapsed 151 days after transplantation. A BM specimen at relapse showed severe fibrosis and progression to overt leukemia, and this patient died of disease at 656 days after transplantation.

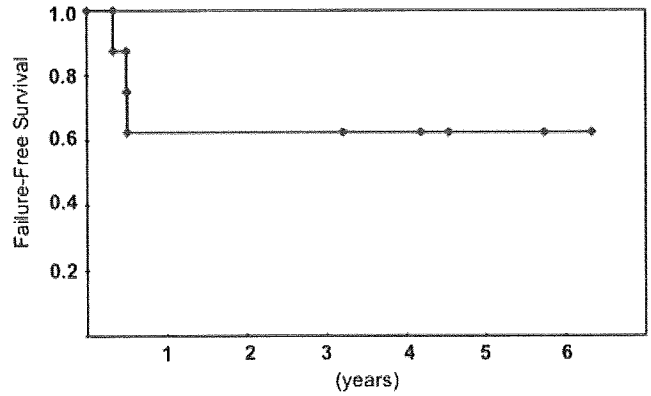

Fig. 2. Kaplan–Meier estimate of failure-free survival of patients who received immunosuppressive therapy. Failure-free survival was calculated from the date of initiating IST to the date of treatment failure as follows; death, no response to IST at 6 months, HSCT, a second course of IST, acquisition of additional chromosomal abnormality, progression to advanced disease, or relapse. The 5-year failure-free survival was $63 \pm 17\%$ (n = 8). Median follow-up was 1,346 days.

Chromosomal Abnormality

There were eight children with chromosomal abnormality in this study. Of those, six received IST and four showed responses to IST, including one with cytogenetic response (UPN 35).

Survival

Of eight children who received IST, three non-responders were considered as treatment failure. No patient died with IST after a median follow-up of 1,346 days; the 5-year FFS was $63 \pm 17\%$ (Fig. 2). Of total, 10 patients are alive after a median follow-up of 1,685 days; the 5-year OS was $90 \pm 9\%$ (Fig. 3).

DISCUSSION

Although HSCT is the curative modality for children with MDS, it may cause severe complications, mortality, and late sequelae. Several reports have shown encouraging results from the use of IST in adults with RA, and the hematological response rate to IST was 30–80% [8–12]. Yoshimi et al. [13] reported on 31 children with hypoplastic RC and normal karyotype or trisomy 8 treated with IST, which resulted in a response rate at 6 months of 71%, 3-year OS of

TABLE II. Comparison of Characteristics Between Responders and Non-Responders to IST

	Responder (n = 5)	Non-responder (n = 3)	*P*-value
Age[a]	2y5m	11y8m	0.03
Gender (male/female)	3:2	1:2	n.s.
Neutrophils[a] ($\times 10^9$/L)	1.27	0.63	n.s.
Hb[a] (g/dl)	8.0	6.2	n.s.
Plt[a] ($\times 10^9$/L)	31.0	20.0	n.s.
No. of cytopenia (tri-/bi-/anemia only)	2:2:1	2:1:0	n.s.
Decreased BM cell content	1/5	2/3	n.s.[b]
Time to IST[a] (day)	42	42	n.s.[b]
Chromosomal abnormality	4/5	2/3	n.s.[b]

[a]Median; [b]Evaluated by Mann–Whitney test and Chi-square test.

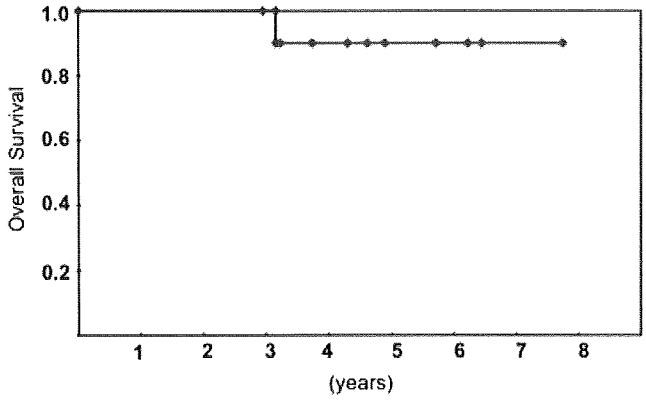

Fig. 3. Kaplan–Meier estimate of overall survival of all evaluable patients. Overall survival was calculated from the date of diagnosis to the date of death or last follow-up. The 5-year overall survival was $90 \pm 9\%$ (n = 11). Median follow-up was 1,685 days.

88%, and 3-year FFS of 57%. In contrast to the larger series by Yoshimi et al. children with RA and karyotypic abnormalities or non-hypoplastic marrow were also enrolled in this study. Overall, 5 of 8 patients (63%) responded to IST, and similar responses were observed in two-thirds of patients with chromosomal abnormalities. Patients whose BM cell content was not low also responded to IST (responder 4, non-responder 1); however, the significance of cellularity in pediatric RA still needs further study. No severe adverse events, disease progression, or death due to any cause after IST was reported. Only one death in this study was due to disease progression after HSCT, which was not related with IST. As a whole, the 5-year OS and FFS were 90% and 63%, which were comparable with the previous study in adult MDS and superior to our previous retrospective analysis of children with RA (4-year OS was 79%) [2]. Therefore, although the number of subjects was limited, we infer from these results that the IST is effective and safe for children with MDS.

The rationale for IST used as treatment of RA is based on previous studies, which suggested that alterations in the immune system might contribute to the pathogenesis in some subgroups of RA [5–7]. Dysregulated T cells are thought to destroy normal hematopoietic cells as bystanders as well as MDS clones [6]. IST can reduce MDS clone-specific T cells and improve normal hematopoiesis, but cytogenetic abnormalities and dysplastic features often persist [9,11,12]. However, in this study one patient showed the disappearance of karyotypic abnormalities. In addition, three of the responders were able to successfully discontinue IST. These results might be explained by the findings that the residual healthy stem cells can compensate for the loss of stem cells after the immune-mediated destruction is interrupted by IST in the setting of aplastic anemia [18,19]. Recovery of healthy hematopoiesis might outstrip MDS clones in these patients. In the patient with monosomy 7 who experienced cytogenetic response another mechanism could be speculated. The investigators from the EWOG-MDS reported that almost half of children with RA had monosomy 7 and they were likely to experience disease progression [3]. In contrast, anecdotal case reports described a decline or disappearance of a monosomy 7 clone [20]. Sloand et al. [21] reported paradoxical responses of monosomy 7 cells to G-CSF. Namely, high concentrations of G-CSF induced significant proliferation of monosomy 7 cells, but survival and proliferation of monosomy 7 cells were inferior to those of diploid cells at lower G-CSF levels. Thus, there is a possibility that the recovery of normal hematopoiesis after the administration of IST might affect the intrinsic level of G-CSF and survival of monosomy 7 cells. However, the interpretation of the present results still needs caution because most patients with RA and monosomy 7, including another case in this study, showed poor prognosis.

Previous studies on IST in adult RA found some factors that could predict good responders to IST, such as younger age, shorter duration of transfusion dependence, HLA-DR15, and presence of an expanded clone of PNH cells [8,10–12]. In this study, age was the only factor that showed a statistically significant difference between responders and non-responders to IST. The European study published by Yoshimi et al. [13] also contained older patients, but the proportion and treatment responses of older patients were not shown. Therefore, the effects of patient age on pathophysiology of pediatric RA and treatment response remain to be elucidated. Of the limited cases who were examined, no patient showed an expansion of PNH clone and only one patient had HLA-DR2 antigen, who responded to IST well. We did not systemically examine the immunological status such as TCR Vbeta repertoire [7] in this study. Clinical trials, including systematic studies on immunological status, are required to investigate prognostic factors more precisely in childhood RA because the sample size in this study was small.

Thus, a significant drawback of our study was small size of registered patients. We assumed that considerable number of patients with RA did not enter this study and might have received HSCT without IST. In fact, retrospective analysis of pediatric MDS in Japan showed that 52 patients with RA were diagnosed by the central morphological review between 1999 and 2006 [22]. Consecutive enrollment on both diagnostic and therapeutic trials would be essential for a future trial. It might allow the determination of biologic parameters that correlated with clinical characteristics.

In conclusion, the present results suggest the efficacy and safety of IST for children with RA. Disease-free status might be expected with IST in a subset of patients. Chromosomal aberration was not an absolute contraindication for IST, whereas using this approach for patients with monosomy 7 has not been substantiated. A larger prospective study including biological surrogate markers for therapeutic interventions would be important to elucidate the clinical characteristics of this rare disease as well as the prognostic factors and mechanism of IST.

ACKNOWLEDGMENT

The authors thank Dr. Y. Nagatoshi, Dr. M. Maeda, Dr. T. Kanazawa, Dr. N. Shiba, Dr. M. Nagasawa, Dr. T. Kusuda, Dr. K. Kokawa, Dr. T. Tsuruta, Dr. S. Oana, Dr. Y. Noguchi, Dr. S. Ikushima, and Dr. A. Watanabe for providing patients' information. We also thank Dr. C. Ogawa and Dr. A. Yoshimi for valuable advice.

REFERENCES

1. Luna-Fineman S, Shannon KM, Atwater SK, et al. Myelodysplastic and myeloproliferative disorders of childhood: A study of 167 patients. Blood 1999;93:459–466.
2. Sasaki H, Manabe A, Kojima S, et al. MDS Committee of the Japanese Society of Pediatric Hematology, Japan. Myelodysplastic syndrome in childhood: A retrospective study of 189 patients in Japan. Leukemia 2001;15:1713–1720.

3. Kardos G, Baumann I, Passmore SJ, et al. Refractory anemia in childhood: A retrospective analysis of 67 patients with particular reference to monosomy 7. Blood 2003;102:1997–2003.
4. Hasle H, Niemeyer CM, Chessells JM, et al. A pediatric approach to the WHO classification of myelodysplastic and myeloproliferative diseases. Leukemia 2003;17:277–282.
5. Selleri C, Maciejewski JP, Catalano L, et al. Effects of cyclosporine on hematopoietic and immune functions in patients with hypoplastic myelodysplasia: In vitro and in vivo studies. Cancer 2002;95:1911–1922.
6. Sloand EM, Mainwaring L, Fuhrer M, et al. Preferential suppression of trisomy 8 compared with normal hematopoietic cell growth by autologous lymphocytes in patients with trisomy 8 myelodysplastic syndrome. Blood 2005;106:841–851.
7. de Vries AC, Langerak AW, Verhaaf B, et al. T-cell receptor Vbeta CDR3 oligoclonality frequently occurs in childhood refractory cytopenia (MDS-RC) and severe aplastic anemia. Leukemia 2008;22:1170–1174.
8. Molldrem JJ, Caples M, Mavroudis D, et al. Antithymocyte globulin for patients with myelodysplastic syndrome. Br J Haematol 1997;99:699–705.
9. Jonásova A, Neuwirtová R, Cermák J, et al. Cyclosporin A therapy in hypoplastic MDS patients and certain refractory anaemias without hypoplastic bone marrow. Br J Haematol 1998;100:304–309.
10. Sauntharajah Y, Nakamura R, Nam JM, et al. HLA-DR15 (DR2) is overrepresented in myelodysplastic syndrome and aplastic anemia and predicts a response to immunosuppression in myelodysplastic syndrome. Blood 2002;100:1570–1574.
11. Shimamoto T, Tohyama K, Okamoto T, et al. Cyclosporin A therapy for patients with myelodysplastic syndrome: Multicenter pilot studies in Japan. Leuk Res 2003;27:783–788.
12. Stadler M, Germing U, Kliche KO, et al. A prospective, randomised, phase II study of horse antithymocyte globulin vs rabbit antithymocyte globulin as immune-modulating therapy in patients with low-risk myelodysplastic syndromes. Leukemia 2004;18:460–465.
13. Yoshimi A, Baumann I, Führer M, et al. Immunosuppressive therapy with anti-thymocyte globulin and cyclosporine A in selected children with hypoplastic refractory cytopenia. Haematologica 2007;92:397–400.
14. Bennett JM, Catovsky D, Daniel MT, et al. Proposals for the classification of the myelodysplastic syndromes. Br J Haematol 1982;51:189–199.
15. Manabe A, Nakahata T. Experiences on MDS and JMML from Japan. In: Lopes LF, Hasle H, editors. Myelodysplastic and myeloproliferative disorders in children. Sao Paulo, Brazil: Lemar Livraria; 2003. pp. 317–324.
16. Vardiman JW, Harris NL, Brunning RD. The World Health Organization (WHO) classification of the myeloid neoplasms. Blood 2002;100:2292–2302.
17. Nagasawa M, Tomizawa D, Tsuji Y, et al. Pancytopenia presenting with monosomy 7 which disappeared after immunosuppressive therapy. Leuk Res 2004;28:315–319.
18. Maciejewski JP, Kim S, Sloand E, et al. Sustained long-term hematologic recovery despite a marked quantitative defect in the stem cell compartment of patients with aplastic anemia after immunosuppressive therapy. Am J Hematol 2000;65:123–131.
19. Führer M, Rampf U, Baumann I, et al. Immunosuppressive therapy for aplastic anemia in children: A more severe disease predicts better survival. Blood 2005;106:2102–2104.
20. Mantadakis E, Shannon KM, Singer DA, et al. Transient monosomy 7: A case series in children and review of the literature. Cancer 1999;85:2655–2661.
21. Sloand EM, Yong AS, Ramkissoon S, et al. Granulocyte colony-stimulating factor preferentially stimulates proliferation of monosomy 7 cells bearing the isoform IV receptor. Proc Natl Acad Sci USA 2006;103:14483–14488.
22. Hirabayashi S, Manabe A, Watanabe S, et al. Myelodysplastic syndrome (MDS) and myeloproliferative disease (MPD) in children: A prospective registration of 222 cases. Blood (ASH Annu Meet Abstr) 2008;112:2678.

LETTERS

Frequent inactivation of A20 in B-cell lymphomas

Motohiro Kato[1,2], Masashi Sanada[1,5], Itaru Kato[6], Yasuharu Sato[7], Junko Takita[1,2,3], Kengo Takeuchi[8], Akira Niwa[6], Yuyan Chen[1,2], Kumi Nakazaki[1,4,5], Junko Nomoto[9], Yoshitaka Asakura[9], Satsuki Muto[1], Azusa Tamura[1], Mitsuru Iio[1], Yoshiki Akatsuka[11], Yasuhide Hayashi[12], Hiraku Mori[13], Takashi Igarashi[2], Mineo Kurokawa[4], Shigeru Chiba[3], Shigeo Mori[14], Yuichi Ishikawa[8], Koji Okamoto[10], Kensei Tobinai[9], Hitoshi Nakagama[10], Tatsutoshi Nakahata[6], Tadashi Yoshino[7], Yukio Kobayashi[9] & Seishi Ogawa[1,5]

A20 is a negative regulator of the NF-κB pathway and was initially identified as being rapidly induced after tumour-necrosis factor-α stimulation[1]. It has a pivotal role in regulation of the immune response and prevents excessive activation of NF-κB in response to a variety of external stimuli[2–7]; recent genetic studies have disclosed putative associations of polymorphic *A20* (also called *TNFAIP3*) alleles with autoimmune disease risk[8,9]. However, the involvement of A20 in the development of human cancers is unknown. Here we show, using a genome-wide analysis of genetic lesions in 238 B-cell lymphomas, that *A20* is a common genetic target in B-lineage lymphomas. A20 is frequently inactivated by somatic mutations and/or deletions in mucosa-associated tissue lymphoma (18 out of 87; 21.8%) and Hodgkin's lymphoma of nodular sclerosis histology (5 out of 15; 33.3%), and, to a lesser extent, in other B-lineage lymphomas. When re-expressed in a lymphoma-derived cell line with no functional *A20* alleles, wild-type A20, but not mutant A20, resulted in suppression of cell growth and induction of apoptosis, accompanied by downregulation of NF-κB activation. The A20-deficient cells stably generated tumours in immunodeficient mice, whereas the tumorigenicity was effectively suppressed by re-expression of A20. In A20-deficient cells, suppression of both cell growth and NF-κB activity due to re-expression of A20 depended, at least partly, on cell-surface-receptor signalling, including the tumour-necrosis factor receptor. Considering the physiological function of A20 in the negative modulation of NF-κB activation induced by multiple upstream stimuli, our findings indicate that uncontrolled signalling of NF-κB caused by loss of A20 function is involved in the pathogenesis of subsets of B-lineage lymphomas.

Malignant lymphomas of B-cell lineages are mature lymphoid neoplasms that arise from various lymphoid tissues[10,11]. To obtain a comprehensive registry of genetic lesions in B-lineage lymphomas, we performed a single nucleotide polymorphism (SNP) array analysis of 238 primary B-cell lymphoma specimens of different histologies, including 64 samples of diffuse large B-cell lymphomas (DLBCLs), 52 follicular lymphomas, 35 mantle cell lymphomas (MCLs), and 87 mucosa-associated tissue (MALT) lymphomas (Supplementary Table 1). Three Hodgkin's-lymphoma-derived cell lines were also analysed. Interrogating more than 250,000 SNP sites, this platform permitted the identification of copy number changes at an average resolution of less than 12 kilobases (kb). The use of large numbers of SNP-specific probes is a unique feature of this platform, and combined with the CNAG/AsCNAR software, enabled accurate determination of 'allele-specific' copy numbers, and thus allowed for sensitive detection of loss of heterozygosity (LOH) even without apparent copy-number reduction, in the presence of up to 70–80% normal cell contamination[12,13].

Lymphoma genomes underwent a wide range of genetic changes, including numerical chromosomal abnormalities and segmental gains and losses of chromosomal material (Supplementary Fig. 1), as well as copy-number-neutral LOH, or uniparental disomy (Supplementary Fig. 2). Each histology type had a unique genomic signature, indicating a distinctive underlying molecular pathogenesis for different histology types (Fig. 1a and Supplementary Fig. 3). On the basis of the genomic signatures, the initial pathological diagnosis of MCL was re-evaluated and corrected to DLBCL in two cases. Although most copy number changes involved large chromosomal segments, a number of regions showed focal gains and deletions, accelerating identification of their candidate gene targets. After excluding known copy number variations, we identified 46 loci showing focal gains (19 loci) or deletions (27 loci) (Supplementary Tables 2 and 3 and Supplementary Fig. 4).

Genetic lesions on the NF-κB pathway were common in B-cell lymphomas and found in approximately 40% of the cases (Supplementary Table 1), underpinning the importance of aberrant NF-κB activation in lymphomagenesis[11,14] in a genome-wide fashion. They included focal gain/amplification at the *REL* locus (16.4%) (Fig. 1b) and *TRAF6* locus (5.9%), as well as focal deletions at the *PTEN* locus (5.5%) (Supplementary Figs 1 and 4). However, the most striking finding was the common deletion at 6q23.3 involving a 143-kb segment. It exclusively contained the *A20* gene (also called *TNFAIP3*), a negative regulator of NF-κB activation[3–7,15] (Fig. 1b), which was previously reported as a candidate target of 6q23 deletions in ocular lymphoma[16]. LOH involving the *A20* locus was found in 50 cases, of which 12 showed homozygous deletions as determined by the loss of both alleles in an allele-specific copy number analysis (Fig. 1b, Table 1 and Supplementary Table 4). On the basis of this finding, we searched for possible tumour-specific mutations of *A20* by genomic DNA sequencing of entire coding exons of the gene in the same series of lymphoma samples (Supplementary Fig. 5). Because two out of the three Hodgkin's-lymphoma-derived cell lines had biallelic *A20* deletions/mutations (Supplementary Fig. 6), 24 primary samples from Hodgkin's lymphoma were also analysed for mutations, where

[1]Cancer Genomics Project, Department of [2]Pediatrics, [3]Cell Therapy and Transplantation Medicine, and [4]Hematology and Oncology, Graduate School of Medicine, University of Tokyo, 7-3-1 Hongo, Bunkyo-ku, Tokyo 113-8655, Japan. [5]Core Research for Evolutional Science and Technology, Japan Science and Technology Agency, 4-1-8, Honcho, Kawaguchi-shi, Saitama 332-0012, Japan. [6]Department of Pediatrics, Graduate School of Medicine, Kyoto University, 54 Kawahara-cho, Shogoin, Sakyo-ku, Kyoto 606-8507, Japan. [7]Department of Pathology, Okayama University Graduate School of Medicine, Dentistry and Pharmaceutical Sciences, 2-5-1 Shikata-cho, Kita-ku, Okayama 700-8558, Japan. [8]Division of Pathology, The Cancer Institute of Japanese Foundation for Cancer Research, Japan, 3-10-6 Ariake, Koto-ku, Tokyo 135-8550, Japan. [9]Hematology Division, Hospital, and [10]Early Oncogenesis Research Project, Research Institute, National Cancer Center, 5-1-1 Tsukiji, Chuo-ku, Tokyo 104-0045, Japan. [11]Division of Immunology, Aichi Cancer Center Research Institute, 1-1 Kanokoden, Chikusa-ku, Nagoya 464-8681, Japan. [12]Gunma Children's Medical Center, 779 Shimohakoda, Hokkitsu-machi, Shibukawa 377-8577, Japan. [13]Division of Hematology, Internal Medicine, Showa University Fujigaoka Hospital, 1-30, Fujigaoka, Aoba-ku, Yokohama-shi, Kanagawa 227-8501, Japan. [14]Department of Pathology, Teikyo University School of Medicine, 2-11-1 Kaga, Itabashi-ku, Tokyo 173-8605, Japan.

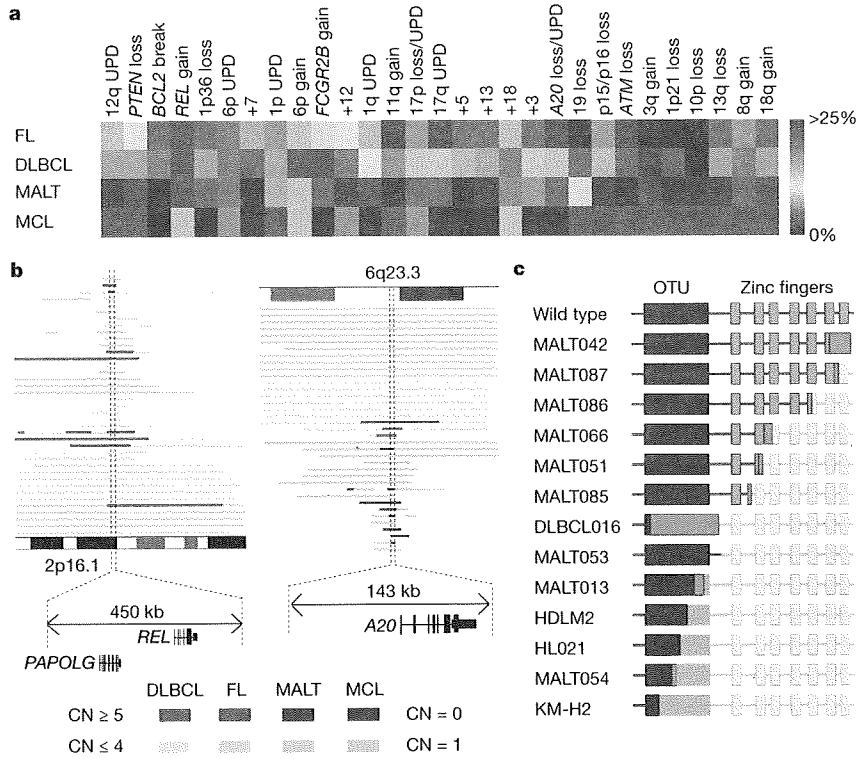

Figure 1 | Genomic signatures of different B-cell lymphomas and common genetic lesions at 2p16-15 and 6q23.3 involving NF-κB pathway genes. **a**, Twenty-nine genetic lesions were found in more than 10% in at least one histology and used for clustering four distinct histology types of B-lineage lymphomas. The frequency of each genetic lesion in each histology type is colour-coded. FL, follicular lymphoma; UPD, uniparental disomy. **b**, Recurrent genetic changes are depicted based on CNAG output of the SNP array analysis of 238 B-lineage lymphoma samples, which include gains at the *REL* locus on 2p16-15 (left panel) and the *A20* locus on 6q23.3 (right panel). Regions showing copy number gain or loss are indicated by horizontal lines. Four histology types are indicated by different colours, where high-grade amplifications and homozygous deletions are shown by darker shades to discriminate from simple gains (copy number ≤4) and losses (copy number = 1) (lighter shades). **c**, Point mutations and small nucleotide insertions and deletions in the *A20* (*TNFAIP3*) gene caused premature truncation of A20 in most cases. Altered amino acids caused by frame shifts are indicated by green bars.

genomic DNA was extracted from 150 microdissected CD30-positive tumour cells (Reed–Sternberg cells) for each sample. *A20* mutations were found in 18 out of 265 lymphoma samples (6.8%) (Table 1), among which 13 mutations, including nonsense mutations (3 cases), frame-shift insertions/deletions (9 cases), and a splicing donor site mutation (1 case) were thought to result in premature termination of translation (Fig. 1c). Four missense mutations and one intronic mutation were identified in five microdissected Hodgkin's lymphoma samples. They were not found in the surrounding normal tissues, and thus, were considered as tumour-specific somatic changes.

In total, biallelic *A20* lesions were found in 31 out of 265 lymphoma samples including 3 Hodgkin's lymphoma cell lines. Quantitative analysis of SNP array data suggested that these *A20* lesions were present in the major tumour fraction within the samples (Supplementary Fig. 7). Inactivation of *A20* was most frequent in MALT lymphoma (18 out of 87) and Hodgkin's lymphoma (7 out of 27), although it was also found in DLBCL (5 out of 64) and follicular lymphoma (1 out of 52) at lower frequencies. In MALT lymphoma, biallelic *A20* lesions were confirmed in 18 out of 24 cases (75.0%) with LOH involving the 6q23.3 segment (Supplementary Fig. 8). Considering the limitation in detecting very small homozygous deletions, *A20* was thought to be the target of 6q23 LOH in MALT lymphoma. On the other hand, the 6q23 LOHs in other histology types tended to be extended into more centromeric regions and less frequently accompanied biallelic *A20* lesions (Supplementary Fig. 8 and Supplementary Table 4), indicating that they might be more heterogeneous with regard to their gene targets. We were unable to analyse Hodgkin's lymphoma samples using SNP arrays owing to insufficient genomic DNA obtained from microdissected samples, and were likely to underestimate the frequency of *A20* inactivation in Hodgkin's lymphoma because we might fail to detect a substantial proportion of cases with homozygous deletions, which explained 50% (12 out of 24) of *A20* inactivation in other histology types. *A20* mutations in Hodgkin's lymphoma were exclusively found in nodular sclerosis classical Hodgkin's lymphoma (5 out of 15) but not in other histology types (0 out of 9), although the possible association requires further confirmation in additional cases.

A20 is a key regulator of NF-κB signalling, negatively modulating NF-κB activation through a wide variety of cell surface receptors and viral proteins, including tumour-necrosis factor (TNF) receptors, toll-like receptors, CD40, as well as Epstein–Barr-virus-associated LMP1 protein[2,5,17,18]. To investigate the role of A20 inactivation in lymphomagenesis, we re-expressed wild-type A20 under a *Tet*-inducible promoter in a lymphoma-derived cell line (KM-H2) that had no functional *A20* alleles (Supplementary Fig. 6), and examined the effect of A20 re-expression on cell proliferation, survival and downstream NF-κB signalling pathways. As shown in Fig. 2a–c and Supplementary Fig. 9, re-expression of wild-type A20 resulted in the suppression of cell proliferation and enhanced apoptosis, and in the concomitant accumulation of IκBβ and IκBε, and downregulation of NF-κB activity. In contrast, re-expression of two lymphoma-derived A20 mutants, $A20^{532Stop}$ or $A20^{750Stop}$, failed to show growth suppression, induction of apoptosis, accumulation of IκBβ and IκBε or downregulation of

Table 1 | Inactivation of A20 in B-lineage lymphomas

Histology	Tissue	Sample	Allele	Uniparental disomy	Exon	Mutation	Biallelic inactivation
DLBCL							5 out of 64 (7.8%)
	Lymph node	DLBCL008	−/−	No	–	–	
	Lymph node	DLBCL016	+/−	No	Ex2	329insA	
	Lymph node	DLBCL022	−/−	No	–	–	
	Lymph node	DLBCL028	−/−	Yes	–	–	
	Lymph node	MCL008*	−/−	Yes	–	–	
Follicular lymphoma							1 out of 52 (1.9%)
	Lymph node	FL024	−/−	No	–	–	
MCL							0 out of 35 (0%)
MALT							18 out of 87 (21.8%)
Stomach							3 out of 23 (13.0%)
	Gastric mucosa	MALT013	+/+	Yes	Ex5	705insG	
	Gastric mucosa	MALT014	+/+	Yes	Ex3	Ex3 donor site>A	
	Gastric mucosa	MALT036	+/−	No	Ex7	delintron6-Ex7†	
Eye							13 out of 43 (30.2%)
	Ocular adnexa	MALT008	−/−	No	–	–	
	Ocular adnexa	MALT017	−/−	No	–	–	
	Ocular adnexa	MALT051	+/−	No	Ex7	1943delTG	
	Ocular adnexa	MALT053	+/+	Yes	Ex6	1016G>A(stop)	
	Ocular adnexa	MALT054	+/−	No	Ex3	502delTC	
	Ocular adnexa	MALT055	−/−	No	–	–	
	Ocular adnexa	MALT066	+/−	No	Ex7	1581insA	
	Ocular adnexa	MALT067	−/−	No	–	–	
	Ocular adnexa	MALT082	−/−	Yes	–	–	
	Ocular adnexa	MALT084	−/−	Yes	–	–	
	Ocular adnexa	MALT085	+/+	Yes	Ex7	1435insG	
	Ocular adnexa	MALT086	+/+	Yes	Ex6	878C>T(stop)	
	Ocular adnexa	MALT087	+/+	Yes	Ex9	2304delGG	
Lung							2 out of 12 (16.7%)
	Lung	MALT042	−/−	No	–	–	
	Lung	MALT047	+/+	Yes	Ex9	2281insT	
Other‡							0 out of 9 (0%)
Hodgkin's lymphoma							7 out of 27 (26.0%)
NSHL	Lymph node	HL10	ND	ND	Ex7	1777G>A(V571I)	
NSHL	Lymph node	HL12	ND	ND	Ex7	1156A>G(R364G)	
NSHL	Lymph node	HL21	ND	ND	Ex4	569G>A(stop)	
NSHL	Lymph node	HL24	ND	ND	Ex3	1487C>A(T474N)	
NSHL	Lymph node	HL23	ND	ND	–	Intron 3§	
	Cell line	KM-H2	−/−	No	–		
	Cell line	HDLM2	+/−	No	Ex4	616ins29bp‖	
Total							31 out of 265 (11.7%)

DLBCL, diffuse large B-cell lymphoma; MALT, MALT lymphoma; MCL, mantle cell lymphoma; ND, not determined because SNP array analysis was not performed; NSHL, nodular sclerosis classical Hodgkin's lymphoma.
* Diagnosis was changed based on the genomic data, which was confirmed by re-examination of pathology.
† Deletion including the boundary of intron 6 and exon 7 (see also Supplementary Fig. 5b).
‡ Including 1 parotid gland, 1 salivary gland, 2 colon and 5 thyroid cases.
§ Insertion of CTC at −19 bases from the beginning of exon 3.
‖ Insertion of TGGCTTCCACAGACACACCCATGGCCCGA.

NF-κB activity (Fig. 2a–c), indicating that these were actually loss-of-function mutations. To investigate the role of A20 inactivation in lymphomagenesis *in vivo*, *A20*- and mock-transduced KM-H2 cells were transplanted in NOD/SCID/γ_c^{null} (NOG) mice[19], and their tumour formation status was examined for 5 weeks with or without induction of wild-type A20 by tetracycline administration. As shown in Fig. 2d, mock-transduced cells developed tumours at the injected sites, whereas the *Tet*-inducible *A20*-transduced cells generated tumours only in the absence of A20 induction (Supplementary Table 5), further supporting the tumour suppressor role of A20 in lymphoma development.

Given the mode of negative regulation of NF-κB signalling, we next investigated the origins of NF-κB activity that was deregulated by A20 loss in KM-H2 cells. The conditioned medium prepared from a 48-h serum-free KM-H2 culture had increased NF-κB upregulatory activity compared with fresh serum-free medium, which was inhibited by re-expression of A20 (Fig. 3a). KM-H2 cells secreted two known ligands for TNF receptor—TNF-α and lymphotoxin-α (Supplementary Fig. 10)[20]—and adding neutralizing antibodies against these cytokines into cultures significantly suppressed their cell growth and NF-κB activity without affecting the levels of their overall suppression after A20 induction (Fig. 3b, d). In addition, recombinant TNF-α and/or lymphotoxin-α added to fresh serum-free medium promoted cell growth and NF-κB activation in KM-H2 culture, which were again suppressed by re-expression of A20 (Fig. 3c, e). Although our data in Fig. 3 also show the presence of factors other than TNF-α and lymphotoxin-α in the KM-H2-conditioned medium—as well as some intrinsic pathways in the cell (Fig. 3a)—that were responsible for the A20-dependent NF-κB activation, these results indicate that both cell growth and NF-κB activity that were upregulated by A20 inactivation depend at least partly on the upstream stimuli that evoked the NF-κB-activating signals.

Aberrant activation of the NF-κB pathway is a hallmark of several subtypes of B-lineage lymphomas, including Hodgkin's lymphoma, MALT lymphoma, and a subset of DLBCL, as well as other lymphoid neoplasms[11,14], where a number of genetic alterations of NF-κB signalling pathway genes[21–25], as well as some viral proteins[26,27], have been implicated in the aberrant activation of the NF-κB pathway[14]. Thus, frequent inactivation of A20 in Hodgkin's lymphoma and MALT and other lymphomas provides a novel insight into the molecular pathogenesis of these subtypes of B-lineage lymphomas through deregulated NF-κB activation. Because A20 provides a

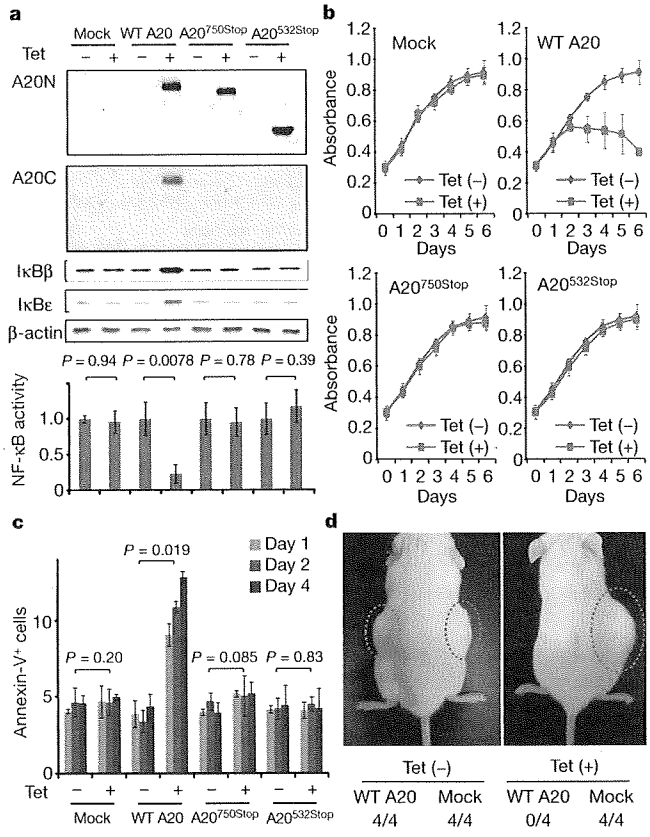

Figure 2 | Effects of wild-type and mutant A20 re-expressed in a lymphoma cell line that lacks the normal *A20* gene. a, Western blot analyses of wild-type (WT) and mutant ($A20^{532Stop}$ and $A20^{750Stop}$) A20, as well as IκBβ and IκBε, in KM-H2 cells, in the presence or absence of tetracycline treatment (top panels). A20N and A20C are polyclonal antisera raised against N-terminal and C-terminal A20 peptides, respectively. β-actin blots are provided as a control. NF-κB activities are expressed as mean absorbance ± s.d. ($n = 6$) in luciferase assays (bottom panel). **b,** Proliferation of KM-H2 cells stably transduced with plasmids for mock and *Tet*-inducible wild-type A20, $A20^{532Stop}$ and $A20^{750Stop}$ was measured using a cell counting kit in the presence (red lines) or absence (blue lines) of tetracycline. Mean absorbance ± s.d. ($n = 5$) is plotted. **c,** The fractions of Annexin-V-positive KM-H2 cells transduced with various *Tet*-inducible A20 constructs were measured by flow cytometry after tetracycline treatment and the mean values (±s.d., $n = 3$) are plotted. **d,** *In vivo* tumorigenicity was assayed by inoculating 7×10^6 KM-H2 cells transduced with mock or *Tet*-inducible wild-type A20 in NOG mice, with (right panel) or without (left panel) tetracycline administration.

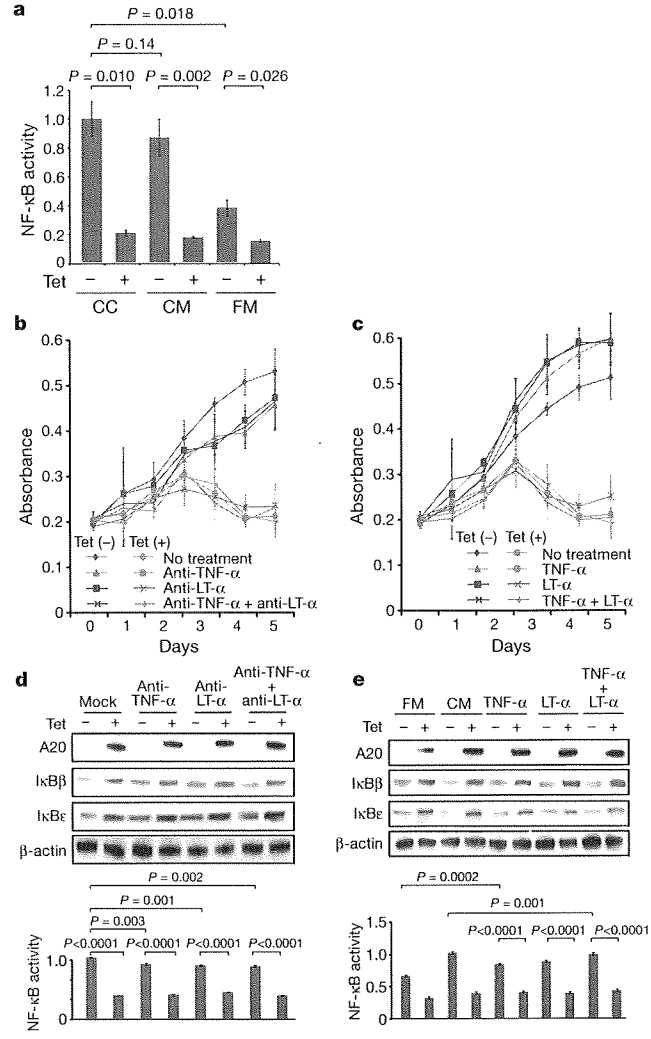

Figure 3 | Tumour suppressor role of A20 under external stimuli. a, NF-κB activity in KM-H2 cells was measured 30 min after cells were inoculated into fresh medium (FM) or KM-H2-conditioned medium (CM) obtained from the 48-h culture of KM-H2, and was compared with the activity after 48 h continuous culture of KM-H2 (CC). A20 was induced 12 h before inoculation in Tet (+) groups. **b, c,** Effects of neutralizing antibodies against TNF-α and lymphotoxin-α (LTα) (**b**) and of recombinant TNF-α and LT-α added to the culture (**c**) on cell growth were evaluated in the presence (Tet (+)) or absence (Tet (−)) of A20 induction. Cell numbers were measured using a cell counting kit and are plotted as their mean absorbance ± s.d. ($n = 6$). **d, e,** Effects of the neutralizing antibodies (**d**) and the recombinant cytokines added to the culture (**e**) on NF-κB activities and the levels of IκBβ and IκBε after 48 h culture with (Tet (+)) or without (Tet (−)) tetracycline treatment. NF-κB activities are expressed as mean absorbance ± s.d. ($n = 6$) in luciferase assays.

negative feedback mechanism in the regulation of NF-κB signalling pathways upon a variety of stimuli, aberrant activation of NF-κB will be a logical consequence of A20 inactivation. However, there is also the possibility that the aberrant NF-κB activity of A20-inactivated lymphoma cells is derived from upstream stimuli, which may be from the cellular environment. In this context, it is intriguing that MALT lymphoma usually arises at the site of chronic inflammation caused by infection or autoimmune disorders and may show spontaneous regression after eradication of infectious organisms[28]; furthermore, Hodgkin's lymphoma frequently shows deregulated cytokine production from Reed–Sternberg cells and/or surrounding reactive cells[29]. Detailed characterization of the NF-κB pathway regulated by A20 in both normal and neoplastic B lymphocytes will promote our understanding of the precise roles of A20 inactivation in the pathogenesis of these lymphoma types. Our finding underscores the importance of genome-wide approaches in the identification of genetic targets in human cancers.

METHODS SUMMARY

Genomic DNA from 238 patients with non-Hodgkin's lymphoma and three Hodgkin's-lymphoma-derived cell lines was analysed using GeneChip SNP genotyping microarrays (Affymetrix). This study was approved by the ethics boards of the University of Tokyo, National Cancer Institute Hospital, Okayama University, and the Cancer Institute of the Japanese Foundation of Cancer Research. After appropriate normalization of mean array intensities, signal ratios between tumours and anonymous normal references were calculated in an allele-specific manner, and allele-specific copy numbers were inferred from the observed signal ratios based on the hidden Markov model using CNAG/AsCNAR software (http://www.genome.umin.jp). *A20* mutations were examined by directly sequencing genomic DNA using a set of primers (Supplementary Table 6). Full-length cDNAs of wild-type and mutant *A20* were introduced into a

lentivirus vector, pLenti4/TO/V5-DEST (Invitrogen), with a *Tet*-inducible promoter. Viral stocks were prepared by transfecting the vector plasmids into 293FT cells (Invitrogen) using the calcium phosphate method and then infected to the KM-H2 cell line. Proliferation of KM-H2 cells was measured using a Cell Counting Kit (Dojindo). Western blot analyses and luciferase assays were performed as previously described. NF-κB activity was measured by luciferase assays in KM-H2 cells stably transduced with a reporter plasmid having an NF-κB response element, pGL4.32 (Promega). Apoptosis of KM-H2 upon A20 induction was evaluated by counting Annexin-V-positive cells by flow cytometry. For *in vivo* tumorigenicity assays, 7×10^6 KM-H2 cells were transduced with the *Tet*-inducible *A20* gene and those with a mock vector were inoculated on the contralateral sides in eight NOG mice[19] and examined for their tumour formation with ($n = 4$) or without ($n = 4$) tetracycline administration. Full copy number data of the 238 lymphoma samples will be accessible from the Gene Expression Omnibus (GEO, http://ncbi.nlm.nih.gov/geo/) with the accession number GSE12906.

Full Methods and any associated references are available in the online version of the paper at www.nature.com/nature.

Received 17 September 2008; accepted 3 March 2009.
Published online 3 May 2009.

1. Dixit, V. M. *et al.* Tumor necrosis factor-α induction of novel gene products in human endothelial cells including a macrophage-specific chemotaxin. *J. Biol. Chem.* **265**, 2973–2978 (1990).
2. Song, H. Y., Rothe, M. & Goeddel, D. V. The tumor necrosis factor-inducible zinc finger protein A20 interacts with TRAF1/TRAF2 and inhibits NF-κB activation. *Proc. Natl Acad. Sci. USA* **93**, 6721–6725 (1996).
3. Lee, E. G. *et al.* Failure to regulate TNF-induced NF-κB and cell death responses in A20-deficient mice. *Science* **289**, 2350–2354 (2000).
4. Boone, D. L. *et al.* The ubiquitin-modifying enzyme A20 is required for termination of Toll-like receptor responses. *Nature Immunol.* **5**, 1052–1060 (2004).
5. Wang, Y. Y., Li, L., Han, K. J., Zhai, Z. & Shu, H. B. A20 is a potent inhibitor of TLR3- and Sendai virus-induced activation of NF-κB and ISRE and IFN-β promoter. *FEBS Lett.* **576**, 86–90 (2004).
6. Wertz, I. E. *et al.* De-ubiquitination and ubiquitin ligase domains of A20 downregulate NF-κB signalling. *Nature* **430**, 694–699 (2004).
7. Heyninck, K. & Beyaert, R. A20 inhibits NF-κB activation by dual ubiquitin-editing functions. *Trends Biochem. Sci.* **30**, 1–4 (2005).
8. Graham, R. R. *et al.* Genetic variants near *TNFAIP3* on 6q23 are associated with systemic lupus erythematosus. *Nature Genet.* **40**, 1059–1061 (2008).
9. Musone, S. L. *et al.* Multiple polymorphisms in the *TNFAIP3* region are independently associated with systemic lupus erythematosus. *Nature Genet.* **40**, 1062–1064 (2008).
10. Jaffe, E. S., Harris, N. L., Stein, H. & Vardiman, J. W. *World Health Organization Classification of Tumours. Pathology and Genetics of Tumours of Hematopoietic and Lymphoid Tissues* (IARC Press, 2001).
11. Klein, U. & Dalla-Favera, R. Germinal centres: role in B-cell physiology and malignancy. *Nature Rev. Immunol.* **8**, 22–33 (2008).
12. Nannya, Y. *et al.* A robust algorithm for copy number detection using high-density oligonucleotide single nucleotide polymorphism genotyping arrays. *Cancer Res.* **65**, 6071–6079 (2005).
13. Yamamoto, G. *et al.* Highly sensitive method for genomewide detection of allelic composition in nonpaired, primary tumor specimens by use of affymetrix single-nucleotide-polymorphism genotyping microarrays. *Am. J. Hum. Genet.* **81**, 114–126 (2007).
14. Jost, P. J. & Ruland, J. Aberrant NF-κB signaling in lymphoma: mechanisms, consequences, and therapeutic implications. *Blood* **109**, 2700–2707 (2007).
15. Durkop, H., Hirsch, B., Hahn, C., Foss, H. D. & Stein, H. Differential expression and function of A20 and TRAF1 in Hodgkin lymphoma and anaplastic large cell lymphoma and their induction by CD30 stimulation. *J. Pathol.* **200**, 229–239 (2003).
16. Honma, K. *et al. TNFAIP3* is the target gene of chromosome band 6q23.3-q24.1 loss in ocular adnexal marginal zone B cell lymphoma. *Genes Chromosom. Cancer* **47**, 1–7 (2008).
17. Sarma, V. *et al.* Activation of the B-cell surface receptor CD40 induces A20, a novel zinc finger protein that inhibits apoptosis. *J. Biol. Chem.* **270**, 12343–12346 (1995).
18. Fries, K. L., Miller, W. E. & Raab-Traub, N. The A20 protein interacts with the Epstein-Barr virus latent membrane protein 1 (LMP1) and alters the LMP1/TRAF1/TRADD complex. *Virology* **264**, 159–166 (1999).
19. Hiramatsu, H. *et al.* Complete reconstitution of human lymphocytes from cord blood $CD34^+$ cells using the NOD/SCID/γ^{null} mice model. *Blood* **102**, 873–880 (2003).
20. Hsu, P. L. & Hsu, S. M. Production of tumor necrosis factor-α and lymphotoxin by cells of Hodgkin's neoplastic cell lines HDLM-1 and KM-H2. *Am. J. Pathol.* **135**, 735–745 (1989).
21. Dierlamm, J. *et al.* The apoptosis inhibitor gene *API2* and a novel 18q gene, *MLT*, are recurrently rearranged in the t(11;18)(q21;q21) associated with mucosa-associated lymphoid tissue lymphomas. *Blood* **93**, 3601–3609 (1999).
22. Willis, T. G. *et al.* Bcl10 is involved in t(1;14)(p22;q32) of MALT B cell lymphoma and mutated in multiple tumor types. *Cell* **96**, 35–45 (1999).
23. Joos, S. *et al.* Classical Hodgkin lymphoma is characterized by recurrent copy number gains of the short arm of chromosome 2. *Blood* **99**, 1381–1387 (2002).
24. Martin-Subero, J. I. *et al.* Recurrent involvement of the *REL* and *BCL11A* loci in classical Hodgkin lymphoma. *Blood* **99**, 1474–1477 (2002).
25. Lenz, G. *et al.* Oncogenic *CARD11* mutations in human diffuse large B cell lymphoma. *Science* **319**, 1676–1679 (2008).
26. Deacon, E. M. *et al.* Epstein-Barr virus and Hodgkin's disease: transcriptional analysis of virus latency in the malignant cells. *J. Exp. Med.* **177**, 339–349 (1993).
27. Yin, M. J. *et al.* HTLV-I Tax protein binds to MEKK1 to stimulate IκB kinase activity and NF-κB activation. *Cell* **93**, 875–884 (1998).
28. Isaacson, P. G. & Du, M. Q. MALT lymphoma: from morphology to molecules. *Nature Rev. Cancer* **4**, 644–653 (2004).
29. Skinnider, B. F. & Mak, T. W. The role of cytokines in classical Hodgkin lymphoma. *Blood* **99**, 4283–4297 (2002).

Supplementary Information is linked to the online version of the paper at www.nature.com/nature.

Acknowledgements This work was supported by the Core Research for Evolutional Science and Technology, Japan Science and Technology Agency, by the 21st century centre of excellence program 'Study on diseases caused by environment/genome interactions', and by Grant-in-Aids from the Ministry of Education, Culture, Sports, Science and Technology of Japan and from the Ministry of Health, Labor and Welfare of Japan for the 3rd-term Comprehensive 10-year Strategy for Cancer Control. We also thank Y. Ogino, E. Matsui and M. Matsumura for their technical assistance.

Author Contributions M.Ka., K.N. and M.S. performed microarray experiments and subsequent data analyses. M.Ka., Y.C., K.Ta., J.T., J.N., M.I., A.T. and Y.K. performed mutation analysis of *A20*. M.Ka., S.Mu., M.S., Y.C. and Y.Ak. conducted functional assays of mutant A20. Y.S., K.Ta., Y.As., H.M., M.Ku., S.Mo., S.C., Y.K., K.To. and Y.I. prepared tumour specimens. I.K., K.O., A.N., H.N. and T.N. conducted *in vivo* tumorigenicity experiments in NOG/SCID mice. T.I., Y.H., T.Y., Y.K. and S.O. designed overall studies, and S.O. wrote the manuscript. All authors discussed the results and commented on the manuscript.

Author Information The copy number data as well as the raw microarray data will be accessible from the GEO (http://ncbi.nlm.nih.gov/geo/) with the accession number GSE12906. Reprints and permissions information is available at www.nature.com/reprints. Correspondence and requests for materials should be addressed to S.O. (sogawa-tky@umin.ac.jp) or Y.K. (ykkobaya@ncc.go.jp).

METHODS

Specimens. Primary tumour specimens were obtained from patients who were diagnosed with DLBCL, follicular lymphoma, MCL, MALT lymphoma, or classical Hodgkin's lymphoma. In total, 238 primary lymphoma specimens listed in Supplementary Table 1 were subjected to SNP array analysis. Three Hodgkin's-lymphoma-derived cell lines (KM-H2, HDLM2, L540) were obtained from Hayashibara Biochemical Laboratories, Inc., Fujisaki Cell Center and were also analysed by SNP array analysis.

Microarray analysis. High-molecular-mass DNA was isolated from tumour specimens and subjected to SNP array analysis using GeneChip Mapping 50K and/or 250K arrays (Affymetrix). The scanned array images were processed with Gene Chip Operation software (GCOS), followed by SNP calls using GTYPE. Genome-wide copy number measurements and LOH detection were performed using CNAG/AsCNAR software[12,13].

Mutation analysis. Mutations in the *A20* gene were examined in 265 samples of B-lineage lymphoma, including 62 DLBCLs, 52 follicular lymphomas, 87 MALTs, 37 MCLs and 3 Hodgkin's-lymphoma-derived cell lines and 24 primary Hodgkin's lymphoma samples, by direct sequencing using an ABI PRISM 3130xl Genetic Analyser (Applied Biosystems). To analyse primary Hodgkin's lymphoma samples in which CD30-positive tumour cells (Reed–Sternberg cells) account for only a fraction of the specimen, 150 Reed–Sternberg cells were collected for each 10 μm slice of a formalin-fixed block immunostained for CD30 by laser-capture microdissection (ASLMD6000, Leica), followed by genomic DNA extraction using QIAamp DNA Micro kit (Qiagen). The primer sets used in this study are listed in Supplementary Table 6.

Functional analysis of wild-type and mutant A20. Full-length cDNA for wild-type *A20* was isolated from total RNA extracted from an acute myeloid leukaemia-derived cell line, CTS, and subcloned into a lentivirus vector (pLenti4/TO/V5-DEST, Invitrogen). cDNAs for mutant A20 were generated by PCR amplification using mutagenic primers (Supplementary Table 6), and introduced into the same lentivirus vector. Forty-eight hours after transfection of each plasmid into 293FT cells using the calcium phosphate method, lentivirus stocks were obtained from ultrafiltration using Amicon Ultra (Millipore), and used to infect KM-H2 cells to generate stable transfectants of mock, wild-type and mutant A20. Each KM-H2 derivative cell line was further transduced stably with a reporter plasmid (pGL4.32, Promega) containing a luciferase gene under an NF-κB-responsive element by electroporation using Nucleofector reagents (Amaxa).

Assays for cell proliferation and NF-κB activity. Proliferation of the KM-H2 derivative cell lines was assayed in triplicate using a Cell Counting Kit (Dojindo). The mean absorption of five independent assays was plotted with s.d. for each derivative line. Two independent KM-H2-derived cell lines were used for each experiment. The NF-κB activity in KM-H2 derivatives for A20 mutants was evaluated by luciferase assays using a PiccaGene Luciferase Assay Kit (TOYO B-Net Co.). Each assay was performed in triplicate and the mean absorption of five independent experiments was plotted with s.d.

Western blot analyses. Polyclonal anti-sera against N-terminal (anti-A20N) and C-terminal (anti-A20C) A20 peptides were generated by immunizing rabbits with these peptides (LSNMRKAVKIRERTPEDIC for anti-A20N and CFQFKQMYG for anti-A20C, respectively). Total cell lysates from KM-H2 cells were separated on 7.5% polyacrylamide gel and subjected to western blot analysis using antibodies to A20 (anti-A20N and anti-A20C), IκBα (sc-847), IκBβ (sc-945), IκBγ (sc-7155) and actin (sc-8432) (Santa Cruz Biotechnology).

Functional analyses of wild-type and mutant A20. Each KM-H2 derivative cell line stably transduced with various *Tet*-inducible A20 constructs was cultured in serum-free medium in the presence or absence of A20 induction using 1 μg ml^{-1} of tetracycline, and cell number was counted every day. 1×10^6 cells of each KM-H2 derivative cell line were analysed for their intracellular levels of IκBβ and IκBε and for NF-κB activities by western blot analyses and luciferase assays, respectively, 12 h after the beginning of cell culture. Effects of human recombinant TNF-α and lymphotoxin-α (210-TA and 211-TB, respectively, R&D Systems) on the NF-κB pathway and cell proliferation were evaluated by adding both cytokines into 10 ml of serum-free cell culture at a concentration of 200 pg ml^{-1}. For cell proliferation assays, culture medium was half replaced every 12 h to minimize the side-effects of autocrine cytokines. Intracellular levels of IκBβ, IκBε and NF-κB were examined 12 h after the beginning of the cell culture. To evaluate the effect of neutralizing TNF-α and lymphotoxin-α, 1×10^6 of KM-H2 cells transduced with both *Tet*-inducible A20 and the NF-κB-luciferase reporter were pre-cultured in serum-free media for 36 h, and thereafter neutralizing antibodies against TNF-α (MAB210, R&D Systems) and/or lymphotoxin-α (AF-211-NA, R&D Systems) were added to the media at a concentration of 200 pg ml^{-1}. After the extended culture during 12 h with or without 1 μg ml^{-1} tetracycline, the intracellular levels of IκBβ and IκBε and NF-κB activities were examined by western blot analysis and luciferase assays, respectively. To examine the effects of A20 re-expression on apoptosis, 1×10^6 KM-H2 cells were cultured for 4 days in 10 ml medium with or without *Tet* induction. After staining with phycoerythrin-conjugated anti-Annexin-V (ID556422, Becton Dickinson), Annexin-V-positive cells were counted by flow cytometry at the indicated times.

***In vivo* tumorigenicity assays.** KM-H2 cells transduced with a mock or *Tet*-inducible wild-type *A20* gene were inoculated into NOG mice and their tumorigenicity was examined for 5 weeks with or without tetracycline administration. Injections of 7×10^6 cells of each KM-H2 cell line were administered to two opposite sites in four mice. Tetracycline was administered in drinking water at a concentration of 200 μg ml^{-1}.

ELISA. Concentrations of TNF-α, lymphotoxin-α, IL-1, IL-2, IL-4, IL-6, IL-12, IL-18 and TGF-β in the culture medium were measured after 48 h using ELISA. For those cytokines detectable after 48-h culture (TNFα, LTα, and IL-6), their time course was examined further using the Quantikine ELISA kit (R&D Systems).

Statistical analysis. Significance of the difference in NF-κB activity between two given groups was evaluated using a paired *t*-test, in which the data from each independent luciferase assay were paired to calculate test statistics. To evaluate the effect of A20 re-expression in KM-H2 cells on apoptosis, the difference in the fractions of Annexin-V-positive cells between Tet (+) and Tet (−) groups was also tested by a paired *t*-test for assays, in which the data from the assays performed on the same day were paired.

Journal of Cellular Physiology

Orderly Hematopoietic Development of Induced Pluripotent Stem Cells via Flk-1$^+$ Hemoangiogenic Progenitors

AKIRA NIWA,[1,2] KATSUTSUGU UMEDA,[1] HSI CHANG,[1] MEGUMU SAITO,[1,2] KEISUKE OKITA,[3] KAZUTOSHI TAKAHASHI,[3] MASATO NAKAGAWA,[3,4] SHINYA YAMANAKA,[3,4] TATSUTOSHI NAKAHATA,[1,2] AND TOSHIO HEIKE[1]*

[1]*Department of Pediatrics, Graduate School of Medicine, Kyoto University, Kyoto, Japan*

[2]*Clinical Application Department, Center for iPS cell Research and Application (CiRA), Institute for Integrated Cell-Material Sciences, Kyoto University, Kyoto, Japan*

[3]*Basic Biology Department, Center for iPS cell Research and Application (CiRA), Institute for Integrated Cell-Material Sciences, Kyoto University, Kyoto, Japan*

[4]*Department of Stem Cell Biology, Institute for Frontier Medical Sciences, Kyoto University, Kyoto, Japan*

Induced pluripotent stem (iPS) cells, reprogrammed somatic cells with embryonic stem (ES) cell-like characteristics, are generated by the introduction of combinations of specific transcription factors. Little is known about the differentiation of iPS cells in vitro. Here we demonstrate that murine iPS cells produce various hematopoietic cell lineages when incubated on a layer of OP9 stromal cells. During this differentiation, iPS cells went through an intermediate stage consisting of progenitor cells that were positive for the early mesodermal marker Flk-1 and for the sequential expression of other genes that are associated with hematopoietic and endothelial development. Flk-1$^+$ cells differentiated into primitive and definitive hematopoietic cells, as well as into endothelial cells. Furthermore, Flk-1$^+$ populations contained common bilineage progenitors that could generate both hematopoietic and endothelial lineages from single cells. Our results demonstrate that iPS cell-derived cells, like ES cells, can follow a similar hematopoietic route to that seen in normal embryogenesis. This finding highlights the potential use of iPS cells in clinical areas such as regenerative medicine, disease investigation, and drug screening.
J. Cell. Physiol. 221: 367–377, 2009.

Because of their pluripotency and potential for self-renewal, embryonic stem (ES) cells have been used in various fields of science, including developmental biology (Evans and Kaufman, 1981). ES cells can differentiate into multiple cell types in a similar way to that observed in vivo. Previous studies using normal or gene-manipulated ES cells have helped to elucidate the process of normal embryogenesis and the genetic mechanisms of some diseases (Lensch and Daley, 2006).

Hematopoietic and endothelial development are regarded as particularly good processes for comparing the potential of ES cells cultivated in vitro with those grown in vivo (Nakano et al., 1994, 1996; Nishikawa et al., 1998). During embryogenesis, the developmental progression to a hematopoietic lineage is closely associated with progression to an endothelial lineage (Shalaby et al., 1997; Wood et al., 1997; Choi et al., 1998; Garcia-Porrero et al., 1998). Both cell lineages emerge from common mesodermal progenitors called hemangioblasts, which are positive for the vascular endothelial growth factor receptor Flk-1 (Flamme et al., 1995; Risau, 1995; Risau and Flamme, 1995; Choi et al., 1998; Huber et al., 2004). Thereafter, the site of hematopoiesis shifts from the yolk sac (primitive hematopoiesis) to the fetal liver, the spleen, and finally to the bone marrow (definitive hematopoiesis), and is accompanied by a change in the type of hemoglobin produced by erythrocytes (Moore and Metcalf, 1970; Matsuoka et al., 2001). Orderly hematopoietic development can be induced from murine and primate ES cells by various culture methods (Doetschman et al., 1985; Leder et al., 1985, 1992; Nakano et al., 1994, 1996; Xu et al., 2001; Umeda et al., 2004, 2006; Shinoda et al., 2007).

ES cells have been proposed as a potential new source of transplantable cells in regenerative medicine. It is anticipated that in the future such ES-derived cells may be used as sources of hematopoietic cells for stem cell transplants, or of mature blood cells for transfusion therapies. Recent studies have already shown that hematopoietic cells derived from murine ES cells overexpressing HoxB4 or Stat5 can replenish the bone marrow of lethally irradiated recipient mice (Kyba et al., 2002, 2003). However, there are various impediments to the clinical application of ES cells. For example, because they are established from the inner-cell masses of blastocysts, ES cells are subject to the controversy surrounding the manipulation of oocytes. Furthermore, the therapeutic use of ES cells from other individuals carries the risk of immunological complications.

Murine and human induced pluripotent stem (iPS) cells have recently been established from somatic cells by retrovirally introducing certain combinations of genes, such as octamer 3/4

The authors indicate no potential conflicts of interest.

Contract grant sponsor: Ministry of Education, Culture, Sports, Science, and Technology of Japan.

*Correspondence to: Toshio Heike, Department of Pediatrics, Graduate School of Medicine, Kyoto University, 54 Kawahara-cho, Shogoin, Sakyo-ku, Kyoto 606-8507, Japan.
E-mail: heike@kuhp.kyoto-u.ac.jp

Received 20 March 2009; Accepted 19 May 2009

Published online in Wiley InterScience (www.interscience.wiley.com.), 26 June 2009.
DOI: 10.1002/jcp.21864

(*Oct3/4*), sex-determining region Y-box 2 (*Sox2*), Krüppel-like factor 4 (*Klf4*), and the v-Myc avian myelocytomatosis viral oncogene homolog (*c-Myc*) (Takahashi and Yamanaka, 2006; Meissner et al., 2007; Okita et al., 2007; Park et al., 2007; Takahashi et al., 2007; Yu et al., 2007; Aoi et al., 2008; Hanna et al., 2008; Nakagawa et al., 2008). The cloned cells display properties of self-renewal and pluripotency similar to ES cells, and yield germ-line adult chimeras. However, because iPS cells are "unnatural" cells that are reprogrammed from once-differentiated cells, their differentiation processes must first be analyzed and compared before any true relationship between iPS and ES cells can be made.

The concept of patient-specific stem cells is of great clinical interest, and has engendered considerable research within the scientific community. The applications of these cells are expected to contribute to patient-oriented disease investigations, drug screenings, toxicology, and transplantation therapies (Jaenisch and Young, 2008). For example, a recent study demonstrated that autologous iPS cells can be used to treat mice with sickle cell anemia (Hanna et al., 2007). Despite such encouraging results, little is known about the in vitro hematopoietic differentiation of iPS cells. In particular, it is currently unclear whether iPS and undifferentiated embryonic cells follow the same process toward hematopoietic commitment.

In this study, we compared the hematopoietic differentiation of iPS and ES cells in vitro during their coculture with OP9 stromal cells (Nakano et al., 1994, 1996; Umeda et al., 2004, 2006; Vodyanik et al., 2005; Shinoda et al., 2007; Vodyanik and Slukvin, 2007). Sequential fluorescence-activated cell sorting (FACS), immunostaining, and reverse transcription (RT)-polymerase chain reaction (PCR) analyses demonstrated that iPS cell-derived hematopoietic and endothelial cells emerge from a common mesodermal progenitor that is positive for Flk-1, as is the case in ES cells and in normal embryogenesis.

Materials and Methods

Generation of iPS cells

Murine iPS cells were established from murine fibroblasts as described previously (Takahashi and Yamanaka, 2006; Okita et al., 2007; Nakagawa et al., 2008). In brief, to generate Nanog-iPS cells (clones 20D17, 38C2, and 38D2), murine embryonic fibroblasts carrying the Nanog-GFP-IRES-Puro^r reporter were incubated in retrovirus-containing supernatants for Oct3/4, Sox2, Klf4, and c-Myc for 24 h. After 2–3 weeks, clones were selected for expansion in medium containing 1.5 μg/ml of puromycin. To generate three-factor (without c-Myc) iPS cells (clone 256H18), murine tail tip fibroblasts (TTFs) were first isolated from adult *Discosoma* sp. red fluorescent protein (DsRed)-transgenic mice. Retrovirus containing supernatants for Oct3/4, Sox2, Klf4, and GFP were then added to the TTF cultures for 24 h. Four days after transduction, TTFs were replated on SIM mouse embryo-derived thioguanine and ouabain-resistant (STO)-derived feeder cells producing leukemia inhibitory factor (LIF; designated as SNL cells). Thirty days after transduction, the colonies were selected for expansion.

Maintenance of cells

The iPS cells and the murine ES cell line D3 were maintained on confluent SNL cells at a concentration of 1×10^4 cells/cm^2 in Dulbecco's modified Eagle's medium (DMEM; Sigma–Aldrich, St. Louis, MO), containing 15% fetal calf serum (FCS; Sigma–Aldrich) and 0.1 μM 2-mercaptoethanol (2ME) (Takahashi and Yamanaka, 2006; Okita et al., 2007; Nakagawa et al., 2008). OP9 stromal cells, which were a kind gift from Dr. Kodama (Osaka University, Osaka), were maintained as reported previously (Umeda et al., 2004).

Antibodies

The primary antibodies used for flow cytometric (FCM) analysis included an unconjugated anti-stage-specific mouse embryonic antigen (SSEA1) mouse monoclonal immunoglobulin M (IgM) antibody (sc-21702; Santa Cruz Biotechnology, Santa Cruz, CA), and the following anti-mouse antibodies from Becton–Dickinson (Franklin Lakes, NJ): unconjugated rat monoclonal anti-E-cadherin, rat monoclonal allophycocyanin (APC)-conjugated anti-c-kit, unconjugated rat monoclonal anti-spinocerebellar ataxia type 1 (Sca1), unconjugated rat monoclonal anti-CD31, biotin-conjugated anti-Flk-1, biotin-conjugated anti-CD34, and biotin-conjugated anti-CD45. Two secondary antibodies against the unlabeled primary antibodies were also from Becton–Dickinson: an APC-conjugated anti-mouse IgM antibody and an APC-conjugated anti-rat IgG antibody.

The primary antibodies used to immunostain the floating erythrocytes included rabbit anti-mouse embryonic hemoglobin (a gift from Dr. Atsumi, Miwa et al., 1991) and rat anti-mouse hemoglobin β (sc31116; Santa Cruz Biotechnology). Cy3-conjugated goat anti-rabbit or anti-rat antibodies (Jackson ImmunoResearch Laboratories, Inc., West Grove, PA) were used as secondary antibodies.

The primary antibodies for immunostaining endothelial cells included anti-mouse antibodies from BD (Becton–Dickinson), an unconjugated anti-VE-cadherin rat monoclonal antibody, an unconjugated anti-CD31 rat monoclonal antibody, and an anti-eNOS rat monoclonal antibody. Horseradish peroxidase (HRP)-conjugated goat anti-rat antibodies (Jackson ImmunoResearch Laboratories, Inc.) were used as secondary antibodies.

Cytostaining

Floating cells were centrifuged onto glass slides using a Shandon Cytospin® 4 Cytocentrifuge (Thermo, Pittsburgh, PA), and analyzed by microscopy after staining with May–Giemsa, myeloperoxidase (MPO), or acetylcholine esterase (Maherali et al., 2007). Staining was performed as described previously (Jackson, 1973; Yang et al., 1999; Xu et al., 2001). For immunofluorescence staining, cells fixed with 4% paraformaldehyde (PFA) were first permeabilized with phosphate-buffered saline (PBS) containing 5% skimmed milk (Becton–Dickinson) and 0.1% Triton X-100, and then incubated with primary antibodies against embryonic or β-major globins, followed by incubation with Cy3-conjugated secondary antibodies. Nuclei were counterstained with 4,6-diamidino-2-phenylindole (Sigma–Aldrich). Fluorescence was detected and images obtained with an AxioCam photomicroscope (Carl Zeiss Vision GmbH, Hallbergmoos, Germany).

FACS

The adherent cells were treated with 0.25% trypsin/ethylenediaminetetraacetic acid (EDTA) and harvested. They were incubated in a new tissue-culture dish (Becton–Dickinson) for 30 min to eliminate adherent OP9 cells (Suwabe et al., 1998). Floating cells were then collected and stained with primary antibodies, followed by incubation with APC-conjugated anti-mouse IgM or anti-rat IgG antibodies. Dead cells were excluded by propidium iodide (Kyba et al., 2002, 2003) staining. Samples were analyzed using a FACSCalibur and Cell Quest software (Becton–Dickinson). Cell sorting with the Flk-1 antibody was performed using a FACSVantage flow cytometer (Becton–Dickinson).

Differentiation of iPS and ES cells

For initial differentiation, iPS or ES cells were treated with 0.25% trypsin/EDTA (Gibco, Grand Island, NY) and transferred onto semi-confluent OP9 cell layers at a concentration of 6×10^3 cells/cm^2 in α-minimum essential medium (α-MEM;

Gibco) supplemented with 10% FCS and 5×10^{-2} μM 2ME and without LIF. After 5 days, the induced cells were treated with 0.25% trypsin/EDTA, and 1.2×10^4 total cells/cm^2 or 1.2×10^3 sorted Flk-1$^+$ cells/cm^2 were transferred onto fresh semi-confluent OP9 cell layers, and cultured thereafter for hematopoietic differentiation in α-MEM supplemented with 10% FCS, 5×10^{-2} μM 2ME, and the following four recombinant growth factors: 100 ng/ml mouse stem-cell factor (mSCF), 4 ng/ml human thrombopoietin (hTPO), 20 ng/ml mouse interleukin 3 (mIL3), and 2 U/ml human erythropoietin (hEPO). These cytokines were kindly provided by Kirin Brewery (Tokyo, Japan).

RNA extraction and RT-PCR analysis

RNA samples were prepared using silica gel membrane-based spin-columns (RNeasy Mini-Kit™; Qiagen, Valencia, CA) and subjected to RT with a Sensiscript-RT Kit™ (Qiagen). All procedures were performed following the manufacturer's instructions. For RT-PCR, yields were adjusted by dilution to produce equal amounts of the glyceraldehyde-3-phosphate dehydrogenase (GAPDH) amplicon. Complementary DNA (cDNA) templates were initially denatured at 94°C for 5 min, followed by 29–35 amplification reactions consisting of 94°C for 15 sec (denaturing), 55–64°C for 15 sec (annealing), and 72°C for 30 sec (extension), with a final extension at 94°C for 7 min. The oligonucleotide primers were as follows: *GAPDH*, 5′-TCC AGA GGG GCC ATC CAC AGT C-3′ and 5′-GTC GGT GTG AAC GGA TTT GGC C-3′ (Baba et al., 2007a); *Rex1*, 5′-AAA GTG AGA TTA GCC CCG AG-3′ and 5′-TCC CAT CCC CTT CAA TAG CA-3′ (Baba et al., 2007a); *Brachyury*, 5′-CAT GTA CTC TTT CTT GCT GG-3′ and 5′-GGT CTC GGG AAA GCA GTG GC-3′ (Ku et al., 2004); *Flk-1*, 5′-CAC CTG GCA CTC TCC ACC TTC-3′ and 5′-GAT TTC ATC CCA CTA CCG AAA G-3′ (Baba et al., 2007a); *Scl*, 5′-ATG GAG ATT TCT GAT GGT CCT CAC-3′ and 5′-AAG TGT GCT TGG GTG TTG GCT C-3′ (Baba et al., 2007a); *Myb*, 5′-CAC CAT TCT GGA CAA TGT TAA GAA C-3′ and 5′-GTA AGG TAG GTG CAT CTA AGC-3′; *Tie1*, 5′-ATA CCC TAG ACT GGC AAG AG-3′ and 5′-TTT TGA CAC TGG CAC TGG A-3′; *Gata1*, 5′-GCT GAA TCC TCT GCA TCA AC-3′ and 5′-TAG GCC TCA GCT TCT CTG TA-3′ (Shimizu et al., 2001); *Gata2*, 5′-GCA ACA CAC CAC CCG ATA CC-3′ and 5′-CAA TTT GCA CAA CAG GTG CCC-3′ (Shimizu et al., 2004); *ε-globin*, 5′-GGA GAG TCC ATT AAG AAC CTA GAC AA-3′ and 5′-CTG TGA ATT CAT TGC CGA AGT GAC-3′ (Hansen et al., 1982); *ζ-globin*, 5′-GCT CAG GCC GAG CCC ATT GG-3′ and 5′-TAG CGG TAC TTC TCA GTC AG-3′ (Leder et al., 1985); *α-globin*, 5′-CTC TCT GGG GAA GAC AAA AGC AAC-3′ and 5′-GGT GGC TAG CCA AGG TCA CCA GCA-3′ (Nishioka and Leder, 1979); *β-globin*, 5′-CTG ACA GAT GCT CTC TTG GG-3′ and 5′-CAC AAC CCC AGA AAC AGA CA-3′ (Konkel et al., 1978); *Oct3/4* (Tg), 5′-AAA AAG CAG GCT CCA CCT TCC CCA TGG CTG GAC ACC-3′ and 5′-AGA AAG CTG GGT TGA TCA ACA GCA TCA CTG AGC TTC-3′ (Takahashi and Yamanaka, 2006); *Sox2* (Tg), 5′-AAA AAG CAG GCT TGT ATA ACA TGA TGG AGA CGG-3′ and 5′-AGA AAG CTG GGT TTC ACA TGT GCG ACA GGG GCA GT-3′ (Takahashi and Yamanaka, 2006); *c-Myc* (Tg), 5′-CAC CAT GCC CCT CAA CGT GAA CTT CAC C-3′ and 5′-TTA TGC ACC AGA GTT TCG AAG CTG TTC G-3′ (Takahashi and Yamanaka, 2006); *Klf4* (Tg), 5′-CAC CAT GGC TGT CAG CGA CGC TCT GCT C-3′ and 5′-ACA TCC ACT ACG TGG GAT TTA AAA-3′ (Takahashi and Yamanaka, 2006).

Real-time quantitative RT-PCR analysis

Forward and reverse primers for *Rex1* and *Flk-1* and the fluorogenic probes were designed according to PerkinElmer guidelines (Primer Express Software; PerkinElmer Life and Analytical Sciences, Boston, MA, http://www.perkinelmer.com), and those of *Brachyury* and *Scl* were described in a previous report (Nakanishi et al., 2009; Redmond et al., 2008). The *GAPDH* primers and probes were purchased from Applied Biosystems (Foster City, CA, http://www.appliedbiosystems.com). Quantitative RT-PCR experiments were performed using the ABI-Prism 7300 system (Applied Biosystems) following the manufacturer's instructions. Quantitative assessment of mRNA expression was performed using a GAPDH internal standard. The expression of each mRNA was compared with each day 0 mRNA expression.

The oligonucleotide primers were as follows: mouse *Rex1*, 5′-AAG CAG GAT CGC CTC ACT GT-3′ and 5′-CCG CAA AAA ACT GAT TCT TGG T-3′ (Baba et al., 2007a); mouse *Brachyury*, 5′-TAC CCC AGC CCC TAT GCT CA-3′ and 5′-GGC ACT CCG AGG CTA GAC CA-3′ (Nakanishi et al., 2009); mouse *Scl*, 5′-CAC TAG GCA GTG GGT TCT TTG-3′ and 5′-GGT GTG AGG ACC ATC AGA AAT CT-3′ (Redmond et al., 2008); mouse Flk-1, 5′-AAG CAG GAT CGC CTC ACT GT-3′ and 5′-CCG CAA AAA ACT GAT TCT TGG T-3′ (Baba et al., 2007a).

Colony-forming assay

Every other day of culture, from days 5 through 15, the adherent cells were treated with 0.25% trypsin/EDTA and harvested. They were incubated in a new tissue-culture dish (Becton–Dickinson) for 30 min to eliminate adherent OP9 cells (Suwabe et al., 1998). Floating cells were then collected and cultured at a concentration of 1×10^4 cells/ml in semi-solid α-MEM supplemented with 1.3% methylcellulose, 30% FCS, 10% bovine serum albumin, 100 μM 2ME, and a mixture of the following growth factors: 10 ng/ml human granulocyte colony-stimulating factor (hG-CSF), 2 U/ml hEPO, 20 ng/ml mIL3, 100 ng/ml mSCF, 100 ng/ml hIL6, and 10 ng/ml hTPO. Colony types were determined according to the criteria described previously (Nakahata and Ogawa, 1982a,b,c) by in situ observation using an inverted microscope. The abbreviations used for the clonogenic progenitor cells were as follows: CFU-Mix, mixed colony-forming units; BFU-E, erythroid burst-forming units; CFU-GM, granulocyte–macrophage colony-forming units; and CFU-G, granulocyte colony-forming units.

Single-cell deposition assay

The single-cell deposition assay was performed as described previously (Nishikawa et al., 1998; Umeda et al., 2006; Shinoda et al., 2007). In brief, single sorted cells were deposited in individual wells of 96-well plates with confluent OP9 layers, and cultured for 5 days in the medium described in the "Differentiation of iPS and ES Cells" Section. Each well was stained with a mixture of anti-CD45, CD41, and Ter119 rat antibodies for hematopoietic lineage detection or anti-VE-cadherin rat-antibodies for endothelial lineage detection, respectively. HRP-conjugated goat anti-rat antibodies (Jackson ImmunoResearch Laboratories, Inc.) were used as secondary antibodies.

Statistics

Statistical analyses were conducted using the Student's *t*-test or the Fisher's exact test. Statistical significance was defined as $P < 0.05$.

Results

iPS cells differentiate into hematopoietic cells in coculture with OP9 stromal cells

We initially compared iPS and ES cells by microscopic examination and FACS analysis. The Nanog-iPS cell lines (Okita